Article:
Al Zamzami, I., Davison, J. and Susmel, L. (2019) Nominal and local stress quantities to design aluminium-to-steel thin welded joints against fatigue. International Journal of Fatigue, 123. pp. 279-295. ISSN: 0142-1123

https://doi.org/10.1016/j.ijfatigue.2019.02.018

Nominal and local stress quantities to design aluminium-to-steel thin welded joints against fatigue

Ibrahim Al Zamzami, ***Buick Davison*** and ***Luca Susmel***

Department of Civil and Structural Engineering, The University of Sheffield,
Mappin Street, Sheffield S1 3JD, United Kingdom

Corresponding Author: Prof. **Luca Susmel**
Department of Civil and Structural Engineering
The University of Sheffield, Mappin Street, Sheffield, S1 3JD, UK
Telephone: +44 (0) 114 222 5073
Fax: +44 (0) 114 222 5700
E-mail: l.susmel@sheffield.ac.uk

ABSTRACT

Welding aluminium to steel to make mechanical joints is possible, but there is, to date, no accepted method for performing the fatigue assessment of such hybrid connections. In this context, the present investigation aims at checking the accuracy of nominal stresses, effective notch stresses, notch-stress intensity factors, and the Modified Wöhler Curve method (applied in conjunction with the Theory of Critical Distances) in estimating fatigue lifetime of butt, cruciform, lap and tee aluminium-to-steel thin welded joints. EWM coldArc® welding technology was used to manufacture the welded specimens that were used for this validation exercise. The samples being tested in the structural laboratory of the University of Sheffield, UK, were manufactured by using AA1050 aluminium and EN10130:1991 steel with main plates thicknesses of 1 mm or 2 mm. The results from this experimental/theoretical investigation demonstrate that all the design methodologies being investigated can be used to perform the fatigue assessment of aluminium-to-steel thin welded joints provided that suitable reference/calibration fatigue curves are used. In the present paper, some quantitative recommendations are given for use in situations of practical interest of the design techniques being considered.

Keywords: aluminium-to-steel welds, nominal stress, local stress, critical plane, critical distance.

Nomenclature

a, b, α, β	fatigue constants for the MWCM's calibration curves
c_0, c_1	constants in the linear regression function
k	negative inverse slope
k_0	negative inverse slope of the torsional fatigue curve
k_τ	negative inverse slope of the modified Wöhler curve
K_I, K_{II}	notch-stress intensity factor (N-SIF) for Mode I and Mode II loading
N_A	reference number of cycles to failure
N_{Ref}	reference number of cycles to failure
N_f	number of cycles to failure
P_S	probability of survival
q	factor for one-sided tolerance limits for normal distribution
r, θ	polar coordinates
r_n	notch root radius
r_{ref}	reference radius
r_{real}	actual root radius in welded joints
R	load ratio ($R=\sigma_{min}/\sigma_{max}$)
t	thickness
T_σ	scatter ratio of the endurance limit range for P_S=90% and P_S=10%
z	weld leg length
σ_{max}, σ_{min}	maximum and minimum stress in the cycle
σ_θ, σ_r	linear-elastic local normal stresses
ρ_w	critical plane stress ratio
λ_1, λ_2, χ_1, χ_2	constants in William's equations
ΔK_I	mode I N-SIF range
$\Delta K_{I,50\%}$	mode I N-SIF range extrapolated at N_A cycles to failure for P_S=50%
$\Delta K_{I,97.7\%}$	mode I N-SIF range extrapolated at N_A cycles to failure for P_S=97.7%
$\Delta\sigma$	stress range
$\Delta\sigma_1$	range of the maximum principal stress
$\Delta\sigma_{A,50\%}$	endurance limit range at N_A cycles to failure for P_S=50%
$\Delta\sigma_{A,97.7\%}$	endurance limit range at N_A cycles to failure for P_S=97.7%
$\Delta\sigma_{nom}$	nominal stress range
$\Delta\sigma_{NS}$	notch stress range
$\Delta\tau_{Ref}$	reference shear stress range extrapolated at N_{Ref} cycles to failure

1. Introduction

For more than a century, engineers have been developing welding technologies in a systematic way as an economical and versatile joining process to replace, where appropriate, the use of mechanical fasteners [1]. Avoidance of fatigue failure associated with the welding process was identified as important from the outset, so that a considerable amount of literature has been published on the effect of the welding process on the durability of weldments subject to fatigue loading. By comparing the robustness of welded and un-welded components made from the same material, a significant reduction in the fatigue strength of welded components is observed [2-4]. This strength reduction is caused by the introduction during welding of residual stresses, imperfections and distortions. Further, localised stress concentrations are common and result in severe stress/strain gradients at the weld toes/roots causing fatigue cracks to initiate in the vicinity of these critical regions [5].

There is a large volume of published studies describing the fatigue behaviour of welded structural details made of either steel or aluminium. These studies consider different fatigue design approaches to estimate the fatigue lifetime of structural components. The available Standards and Codes of Practice [6, 7, 8] suggest different design methods including those based on the use of nominal stress as well as of effective notch stresses. The nominal stress approach, which is undoubtedly the simplest and most widely used design methodology, estimates fatigue strength by simply selecting an appropriate S-N curve amongst those provided by the Standard Codes for each specific welded detail [9]. However, the nominal stress approach is limited to designing only those specific welded geometries for which a reference S-N curve is available.

A more advanced method recommended by the International Institute of Welding (IIW) [6] is the so-called effective notch stress approach. This method estimates the fatigue strength of welded connections by assuming that weld toes/roots behave like rounded notches with a radius equal to 1 mm for a plate thickness larger than or equal to 5 mm [6] and to 0.05 mm for a main plate thickness lower than 5 mm [10-15].

Another method that can be successfully used to assess the fatigue strength of welded joints is the so-called Notch-Stress Intensity Factor (N-SIF) approach [16, 17]; this fatigue assessment technique is based on William's solutions [18] for V-notches having a tip radius equal to zero. Recently, attention has been focused on extending the use of the Theory of Critical Distances (TCD) to the fatigue assessment of welded joints [19, 20]. The TCD groups together a number of local stress-based approaches where fatigue damage in the presence of any kind of stress concentrator is estimated by directly post-processing the linear-elastic stress fields acting on the materials in the vicinity of the assumed crack initiation locations. The TCD provides very accurate estimations of the fatigue lifetime of welded components and requires less computational effort than the effective notch stress approach [19, 21].

As reducing the overall weight of vehicles leads to a reduction in fuel consumption [22], current developments in the transportation industry have sought to replace the ferrous metallic components with lightweight structural metals such as aluminium alloys. As a result, significant attention has been paid in recent years to develop welding technologies capable of joining aluminium to steel metallurgically to achieve not only strong hybrid joints, but also higher productivity [23-26]. Because aluminium alloys and steel have incompatible thermal and physical properties and also different metallurgical characteristics, conventional fusion welding becomes problematic. During welding the formation of intermetallic phases (Fe-Al) deteriorates the strength of the joints by introducing brittle layers at the interface between the two materials [27-32]. To overcome this problem, in recent years different welding techniques have been developed and optimised, with welding technology coldArc® commercialised by EWM (www.ewm-group.com) being, to date, the most advanced solution which provides excellent arc-stability and highly controlled heat input [33, 34].

Understanding of the fatigue behaviour of welded joints made using dissimilar materials (and, in particular, aluminium alloys and steel) is very limited. Before investigating the fatigue behaviour of aluminium-to-steel welded joints, it is important to understand the static behaviour of such connections. A recent experimental study [35] was carried out in order to investigate the static behaviour of aluminium-to-steel thin welded joints with different geometrical configurations - including butt-welded joints (with weld seam inclination angles ranging between 0° and 60°), cruciform connections, and lap joints. This study highlighted that, regardless of the joint configuration or the angle of inclination, the fracture of these hybrid connections always took place in the aluminium heat affected zone. This experimental finding confirmed that Eurocode 9 [36] can be used to design aluminium-to-steel welded joints with a high level of accuracy [35].

The present paper reports the findings of an experimental, theoretical, and numerical study on the fatigue behaviour of aluminium-to-steel thin welded joints under uniaxial cyclic loading. The ultimate aim of the present investigation is to recommend appropriate design strategies suitable for accurately performing the fatigue assessment of aluminium-to-steel hybrid welded connections.

2. Experimental Procedure

An experimental investigation was designed to generate a large number of data suitable for checking the accuracy and reliability of different design approaches in estimating fatigue strength of steel-to-aluminium thin welded joints. The details of this extensive experimental work are summarised in the following sub-sections.

2.1 Materials

The materials used in this investigation were aluminium alloy AA1050 (containing 99.5% of aluminium) and a zinc-coated cold-rolled low carbon steel manufactured in accordance with EN 10130:1991. The ultimate tensile strength of these two materials were 120 MPa and 410 MPa, respectively, with Young's modulus equal to 71 GPa for the aluminium alloy and to 210 GPa for the steel. The thickness of the zinc coating on the steel sheets was measured to be 25 μm.

The 1 mm diameter filler wire used in the welding process was made of AA4043 aluminium alloy. During welding, pure argon was used as shielding gas. Two different sheet thicknesses (i.e., 1 mm and 2 mm) were used to manufacture the fatigue specimens to be tested under load ratios, R, equal to -1, 0.1, and 0.5. The chemical compositions of the materials used in this investigation are summarised in Table 1.

2.2 Welding of the fatigue specimens

Various welded joint configurations (see Fig. 1) were manufactured by an experienced technician using an EWM alpha Q551 pulse machine. Welding technology EWM coldArc® is a modified short-arc process that has gap bridge capabilities and can provide effective control over the heat input and the metal transfer. As far as very thin materials are concerned, the low heat input allows them to be welded together without causing burn-through. The coldArc® process is able to joint hybrid sheets with a thickness as thin as 0.3 mm and 0.7 mm using automated and manual welding machines, respectively. The unique features of the coldArc® technology make it suitable for fabricating aluminium-to-steel thin joints, provided that the steel sheet is pre-coated with zinc to prevent the formation of hard and brittle intermetallic phases at the interface between the two materials.

EWM provides very detailed welding parameter envelopes for different welding combinations and different thicknesses. For the 1 mm thick sheets, the welding parameters were set as follows: arc voltage equal to 15.3 V, current to 54 A, wire feed to 5 m/min; for the 2 mm thick plates the parameters were: arc voltage equal to 18.2 V, current to 88 A, wire feed to 7.9 m/min. The specimens were manufactured by welding aluminium and steel sheets having width equal to 70 mm. The welded samples were subsequently cut down to 50 mm width to eliminate any undesirable defects formed at the edges during the welding process.

2.3 Investigated welded geometries

Four different geometrical configurations were manufactured and prepared for fatigue testing, including butt, cruciform, lap and tee-welded joints (Fig. 1).

The butt joints were fabricated by using a single weld (Fig. 1a). It is important to point out here that the galvanised steel sheets were zinc-coated solely on the top and bottom surfaces, leaving

the edges with no zinc. Thus, the butt-welded joints were characterised by a lack of adhesion between the steel and the aluminium. This lack of adhesion resulted in a gap between the two materials, so that the overall mechanical strength was due to the weld that acted as a bridge holding the two materials together (see Fig. 1a).

The manufacturing of the cruciform welded joints was performed using a welding jig specifically designed to ensure that the top and bottom stiffeners were aligned and welded as straight as possible (Fig. 1b). This effectively minimised any detrimental phenomena associated with eccentricity.

Because the steel edges were not galvanised, producing the lap joint in the traditional form was not possible. Accordingly, the lap joints being tested were manufactured by bending the steel sheet at 90°. As can be seen in Fig. 1c, this allowed the weld seam to be placed between the galvanised steel and the aluminium. As will be discussed below in detail, due to the specific geometrical features characterising these welded specimens, this particular shape was taken into account explicitly when determining the local stress fields being used to assess fatigue strength.

Finally, the tee-welded joints were prepared with the stiffener made of aluminium and the main plate made of steel (Fig. 1d). To prevent the main plate from bending during welding, all the tee-welded joints were manufactured by using sheets having thickness equal to 2 mm.

2.4 Fatigue testing

The fatigue tests were run at room temperature by using a 100 kN capacity MAYSE dynamic machine. The specimens were tested in the as-welded condition under a frequency of 10 Hz. Prior to fatigue testing, the clear distance between the weld seam regions and the hydraulic grips was set to approximately 20 mm for all the welded configurations. This allowed us to minimise any secondary bending effect. As to this aspect, it is important to highlight that no external fixtures were used to support the specimens during testing. This is because all the specific supporting devices being available in our testing laboratory were seen to somehow affect the way the loading was applied to the thin welded joints. Accordingly, in order to generate sets of valid fatigue results, the different welded geometries were tested as detailed in what follows.

For the butt and cruciform welded joints, two different plate thicknesses were used: 1 mm for a load ratio equal to 0.1, and 2 mm for a load ratio equal to -1. Under fully-reversed loading (i.e., $R=\sigma_{min}/\sigma_{max}=-1$), the 2 mm thickness plates provided sufficient stiffness to prevent, under the compressive part of the cyclic loading, secondary bending from affecting the fatigue results being generated.

In contrast, since the lap joints were rather long, the excessive deflection due to secondary bending made it impossible for this specific welded geometry to be tested under fully-reversed

axial loading. Accordingly, the lap joints with thickness equal to 1 mm were tested under R=0.1, whereas those with thickness equal to 2mm under R=0.5.
Finally, the tee-welded joints with thickness equal to 2 mm were tested by setting the load ratio equal to -1 as well as to 0.1.

3. Lifetime estimation using the nominal stress approach

The nominal stress-based approach is one of the most widely used methods that is employed in situations of practical interest to perform the fatigue assessment of welded components. This approach postulates that the required design stresses have to be calculated according to classic continuum mechanics by directly referring to the nominal cross-sectional area. Nominal stresses are determined without taking into account localised stress raising phenomena due to the presence of the weld toe as these phenomena are already included in the reference fatigue design curves being provided by the available design codes - such as Eurocode 9 (EC9) [7], Eurocode 3 (EC3) [8], and the IIW Recommendations [6]. Consequently, the selection of an appropriate design curve is essential to ensure that accurate fatigue design is achieved [6, 37-40]. Although the nominal stress approach is simple and accurate, unfortunately, it cannot be used to design complex/non-standard welded details [37] unless the specific design curve being needed is generated by running appropriate experiments.
Turning to aluminium-to-steel welded joints, currently, there is no guidance for the static and fatigue assessment of these hybrid welded connections. As far as static failures are concerned, examination of the state of the art demonstrates that, so far, the international scientific community has focused its attention mainly on studying the existing interactions amongst welding technologies, material microstructural features and ultimate tensile strength [24, 34, 35, 41-46]. In this context, in a recent investigation [35] it was observed that *static* fracture of aluminium-to-steel welded joints always occurs in the heat affected zone on the aluminium side. In contrast, the direct inspection of the fracture surfaces generated under *fatigue* loading revealed that the fatigue breakage of aluminium-to-steel welded joints always took place at the interface between weld toe and aluminium plate (Fig. 2). This strongly supports the idea that in aluminium-to-steel welded connections the crack initiation process was favoured by localised stress concentration phenomena occurring in the weld seam region.
Based on the above experimental evidence, the hypothesis was formed that aluminium-to-steel welded joints behave like conventional welded connections so that, in situations of practical interest, they can be designed against fatigue by directly using the nominal stress approach along with the design curves recommended by EC9 [7], EC3 [8] and the IIW [6].
The results of the re-analyses performed in terms of nominal stresses are summarised in Tables 2 to 5. These tables were populated by post-processing the experimental results,

expressed in terms of nominal stress ranges, under the hypothesis of a log-normal distribution of the number of cycles to failure for each stress level, with the confidence level being set equal to 95% [39]. The ranges of the endurance limits listed in Table 6 were extrapolated at $2 \cdot 10^6$ cycles to failure for a probability of survival, P_s, equal to 50% and 97.7%. Figure 3 presents the same results in log-log Wöhler diagrams, where, for the different welded configurations being investigated, the nominal stress range, $\Delta\sigma_{nom}$, is plotted against the number of cycles to failure, N_f. In addition, the design curves recommended by EC9 [7], EC3 [8] and the IIW [9] for each welded geometry are also plotted in the charts of Fig. 3, which allows the experimental results to be compared directly with the standard design curves.

Table 6 and the Wöhler diagrams of Figs 3a to 3c make it evident that the values of the negative inverse slope, k, determined for the investigated welded configurations were much larger not only than the value of 3 recommended by the IIW [9], but also than the value of 3.4 suggested by EC9 [7]. This is not surprising since the negative inverse slopes provided by the available design codes were determined by re-analysing a large number of experimental results generated by testing welded joints that were thick and stiff - i.e., welded connections with thickness much larger than 5 mm. In contrast, the experimental fatigue curves experimentally determined by testing thin and flexible welded connections are seen to be characterised by a negative inverse slope that varies in the range 3-6 [47]. This is the reason why Sonsino et al. [47] recommend performing the fatigue assessment of thin welded joints via fatigue curves that have the same endurance limit (at 2 million cycles) as the one provided by the pertinent standard codes and negative inverse slope invariably equal to 5.

By applying the strategy recommended by Sonsino and co-workers to assess the fatigue strength of thin welded joints [47], the use of the modified EC9 design curves (grey dotted line in Figs 3a to 3c) and the modified IIW design curves (black dashed line in Figs 3a to 3c) lead to a more conservative estimation of the fatigue lifetime of aluminium-to-steel welded joints. In particular, as per the Wöhler diagrams of Figs 3a to 3c, the modified IIW design curves were seen to provide conservative fatigue lifetime estimations for all the welded configurations. In contrast, the modified EC9 curves were seen to result in conservative fatigue strength predictions in all cases except for butt joints (Fig. 3a).

Turning to the non-load carrying fillet tee-welded joints (Fig. 3d), the steel plates were subjected to fatigue loading whereas the aluminium plates acted solely as stiffeners. Although the tee-welded joints were 2 mm thick (i.e., thin joints), the negative inverse slope was kept the same as suggested by the design codes for plates with thickness larger than 5 mm, with this still resulting in conservative estimations. This means that the use of a k value equal to 5 as suggested by Sonsino et al. for thin plates [47] resulted in an even higher level of conservatism in estimating the fatigue lifetime of the tee-welded joint (Fig. 3d).

To summarise, using the nominal stress approach, the fatigue behaviour of aluminium-to-steel butt (Fig. 3a), cruciform (Fig. 3b), and lap (Fig. 3c) welded joints can be assessed by treating the joints as conventional aluminium-to-aluminium welded joints, with a higher degree of accuracy being reached by setting, as suggested by Sonsino et al. [47], the negative inverse slope equal to 5. In contrast, as far as hybrid tee-welded joints are concerned (Fig. 1d), these connections can be treated as standard steel-to-steel joints and designed by following either the IIW recommendations or EC3, with this being done without the need for adjusting the value of the negative inverse slope.

4. Lifetime estimation in terms of effective notch stresses

The effective notch stress approach is a well-known methodology that is widely used in industry to determine the fatigue strength of welded details. This approach is also the most advanced design methodology recommended by the IIW. This method estimates fatigue strength by using linear-elastic notch stresses calculated by fictitiously rounding the weld toes or the weld roots [9, 12, 48]. By taking full advantage of the micro-support theory formulated by Neuber to model sharp cracks, Radaj [49-53] developed the effective notch stress approach by proposing to use a fictitious radius, r_{ref}, equal to 1 mm, with this value for r_{ref} being recommended to be adopted solely to assess welded connections with thickness larger than 5 mm (see Fig. 4a). In contrast, for welded details with thickness lower than 5 mm, weld toes/roots should be rounded by adopting a fictitious radius equal to 0.05 mm [13, 49, 54-57]. As far as aluminium welded joints with thickness larger than 5 mm are concerned, the IIW [6] recommends to assess their fatigue strength by using a design curve having notch stress endurance limit range, $\Delta\sigma_{A,97.7}$, equal to 71 MPa (extrapolated at 2.10^6 cycles to failure for a probability of survival, P_s, equal 97.7%) and negative inverse slope, k, equal to 3. In contrast, an aluminium welded detail with thickness lower than 5 mm should be designed against fatigue by using the FAT180 design curve, i.e., a fatigue curve having k equal to 5 and $\Delta\sigma_{A,97.7}$ equal to 180 MPa (with this endurance limit being again determined at 2.10^6 cycles to failure for a P_s equal 97.7%) [12, 47].

In order to post-process the experimental data according to the effective notch stress approach, the stress analysis was carried out by using FE code ANSYS® to solve linear-elastic bi-dimensional models (Fig. 5a). Since the welded joints being investigated had thickness lower than 5 mm, design notch stresses were calculated by rounding the weld toes of the lap and cruciform joints and the roots of the butt joints by setting the reference radius, r_{ref} , equal to 0.05 mm. The mesh density in the vicinity of the fictitious fillet radii was gradually refined until convergence occurred.

The experimental results post-processed according to the effective notch stress approach, for the butt (Fig.1a), cruciform (Fig.1b) and lap welded joints (Fig.1c) are listed in Table 2-4. The

same results are also plotted in the log-log Wöhler diagrams of Figs 4c, 4d and 4e. Table 6 summarises the results from the statistical reanalysis in terms of negative inverse slope and endurance limit range, $\Delta\sigma_A$, extrapolated at $2{\cdot}10^6$ cycles to failure for a probability of survival, P_s, equal to 50% and to 97.7%.

Turning back to the stress analysis aspects, as far as the tee-welded joints were concerned, the maximum stress was seen to occur at the interface between the aluminium weld and the steel plate rather than at the weld toe (Fig.4b). Accordingly, since for this specific configuration the notch stress approach could not be applied rigorously, the tee-welded joints (Fig.1d) were then excluded from the present re-analysis.

The S-N charts of Figs 4c to 4e demonstrate that the use of the FAT180 curve recommended by Sonsino et al. to design aluminium-to-aluminium welded joints [12, 47] was not capable of satisfactorily modelling the fatigue behaviour of the hybrid welded specimens being tested, with its use resulting in a large degree of non-conservatism.

In order to determine a fatigue curve suitable for designing aluminium-to-steel welded joints according to the notch stress approach, all the data generated were then re-analysed together. By so doing, as per the Wöhler diagram of Fig. 4f, the most appropriate design curve to be used to model the fatigue strength of our aluminium-to-steel thin welded specimens was seen to be the one having endurance fatigue limit range equal to 90 MPa (at $2{\cdot}10^6$ cycles to failure for P_s equal to 97.7%) and inverse negative slope equal to 5.

To conclude, a recommended value for the endurance limit of 90 MPa was derived in accordance with the IIW numeric system [6], whereas the value for the negative slope was chosen according to the value that is recommended by Sonsino et al. to design thin and flexible welded joints [47].

5. Lifetime estimation in terms of the N-SIFs approach

By taking full advantage of the classic analytical solution devised by Williams [18], Verreman and Nie [58] laid the foundations of the Notch-Stress Intensity Factor (N-SIF) approach [59, 60]. In order to understand the fundamental idea on which the N-SIF approach is based, consider the joint sketched in Fig. 6a. In this connection the toe radius, r_n, of the weld seam is assumed to be invariably equal zero. According to the system of coordinates as defined in Fig. 6a, the linear elastic stress field in the vicinity of the weld seam can be described analytically via the following relationships for Mode I and Mode II loading, respectively [61, 62]:

$$\begin{Bmatrix}\sigma_\theta\\ \sigma_r\\ \tau_{r\theta}\end{Bmatrix} = \frac{1}{\sqrt{2\pi}}\frac{r^{\lambda_i-1}K_I}{(1+\lambda_i)+\chi_i(1-\lambda_i)}\left[\begin{Bmatrix}(1+\lambda_i)\cos(1-\lambda_i)\theta\\ (3-\lambda_i)\cos(1-\lambda_i)\theta\\ (1-\lambda_i)\sin(1-\lambda_i)\theta\end{Bmatrix} + \chi_i\begin{Bmatrix}\cos(1+\lambda_i)\theta\\ -\cos(1+\lambda_i)\theta\\ \sin(1+\lambda_i)\theta\end{Bmatrix}\right] \quad (1)$$

$$\begin{Bmatrix}\sigma_\theta\\ \sigma_r\\ \tau_{r\theta}\end{Bmatrix}=\frac{1}{\sqrt{2\pi}}\frac{r^{\lambda_i-1}K_{II}}{(1+\lambda_i)+\chi_i(1-\lambda_i)}\left[\begin{Bmatrix}(1+\lambda_i)\cos(1-\lambda_i)\theta\\ (3-\lambda_i)\cos(1-\lambda_i)\theta\\ (1-\lambda_i)\sin(1-\lambda_i)\theta\end{Bmatrix}+\chi_i\begin{Bmatrix}\cos(1+\lambda_i)\theta\\ -\cos(1+\lambda_i)\theta\\ \sin(1+\lambda_i)\theta\end{Bmatrix}\right] \quad (2)$$

In Eqs (1) and (2) λ_i and χ_i (i=1, 2) are parameters depending on the opening angle of the V-notch [64]. K_I and K_{II} are instead the N-SIFs for Mode I and Mode II loading, respectively, and can be determined according to the following definitions [62, 63]:

$$K_I=\sqrt{2\pi}\lim_{r\to 0}(\sigma_\theta)_{\theta=0}r^{1-\lambda_1} \quad (3)$$

$$K_{II}=\sqrt{2\pi}\lim_{r\to 0}(\sigma_\theta)_{\theta=0}r^{1-\lambda_2} \quad (4)$$

Given this sophisticated theoretical framework, Verreman and Nie [58] argued that the stress intensity factors associated with the singular stress fields at the weld toes could directly be used to model the crack initiation process in welded connections subjected to in-service fatigue loading. A few years later, Lazzarin, Tovo and Livieri [62-65] further developed this approach by taking full advantage of the fact that, in welded connections, Mode II stress fields are never singular, with this holding true even if the weld seams are modelled as sharp V-notches with root radius invariably equal to zero. This is a consequence of the fact that the opening angle of the weld seams used to manufacture real structural joints is always larger than 100°, with the most common value being 135°. Accordingly, back at the end of the 1990s, Lazzarin and Tovo [64, 65] postulated that the fatigue strength of welded joints could successfully be assessed directly in terms of Mode I N-SIF ranges (i.e., by solely considering the singular part of the analytical solution). The accuracy and reliability of this approach was checked against a large number of experimental data generated by testing steel non-load-carrying fillet welds having thickness varying in the range 13 mm-100 mm [66, 67]. Subsequently, Lazzarin and Livieri [68] extended the use of the N-SIF approach also to the fatigue assessment of aluminium welded connections. This was done by considering non-load-carrying/load-carrying fillet joints as well as tee-welded connections with thickness ranging from 3 mm up to 24 mm.
Such a massive body of research work has resulted in two fatigue design curves that can be used in situations of practical interest to perform the fatigue assessment of both steel-to-steel and aluminium-to-aluminium welded connections. In particular, the master curve to be used to design against fatigue steel weldments is characterised by a Mode I N-SIF range at $5\cdot10^6$ cycles to failure, ΔK_I, equal to 155 MPa·mm$^{0.326}$ (P_S=97.7%) and a negative inverse slope, k, equal to 3.2. In contrast, the reference curve recommended to be used to design aluminium welded connections against fatigue has ΔK_I at $5\cdot10^6$ cycles to failure equal to 74 MPa·mm$^{0.326}$ (for P_S=97.7%) and k equal to 4.

The experimental results generated by testing the lap (Fig. 1c) and cruciform (Fig. 1b) aluminium-to-steel welded joints were post-processed in terms of Mode I N-SIF ranges. The butt joints (Fig. 1a) were instead excluded from this re-analysis, since the master curve proposed by Lazzarin and Livieri [68] is only suitable for estimating the fatigue strength of fillet welded joints with an opening angle of 135°.

As to the numerical stress analysis done using commercial software ANSYS®, the weld seams of the hybrid joints were all modelled by setting the weld toe radius equal to zero, with the weld leg attached to the steel stiffener being set equal to the weld leg attached to the aluminium plate (see Fig.6b). The numerical procedure proposed by Tovo and Lazzarin was then followed to mesh the FE models as well as to calculate the associated N-SIF values [64, 66].

The results obtained from the statistical re-analysis by post-processing the lap and cruciform welded configurations according to the N-SIFs approach are listed in Tables 3 and 4 and plotted in Fig. 6c in the form of ΔK_I vs. N_f log-log Wöhler diagrams. Table 6 summarises the values of the negative inverse slope, k, and the Mode I N-SIF ranges (for P_S equal to 50% and 97.7%) determined at $5 \cdot 10^6$ cycles to failure.

Fig. 6c makes it evident that Lazzarin and Livieri's master curve was not suitable for modelling the fatigue strength of the aluminium-to-steel hybrid joints tested in this work, with its use resulting in non-conservative estimates. This may be ascribed to the fact that, since the aluminium alloy used to manufacture the welded specimens of Fig. 1 belonged to the 1000 series, its fatigue strength was much lower than the one characterising the aluminium-to-aluminium welded joints that were used by Lazzarin and Livieri themselves to derive their master curve. Furthermore, the parent material thickness used in the present investigation was equal either to 1 mm or to 2 mm. In contrast, the welded joints used to determine the master curve had thicknesses ranging between 3 mm and 24 mm [68]. Another important aspect is that, for thin welded joints, ΔK_I may not be able to effectively model the characteristics of the local linear-elastic stress fields because their features can be described accurately provided that higher order terms (such as, for instance, the T-stress) are effectively taken into account. All these differences and aspects could then explain the reason why the fatigue strength (and the associated negative inverse slope) of the investigated hybrid welded connections was seen to be slightly lower than the one predicted by Lazzarin and Livieri's master curve.

In order to propose a design curve suitable for estimating the fatigue strength of thin aluminium-to-steel welded joints also in terms of Mode I N-SIF ranges, the full set of data for the lap and cruciform welded joints were reanalysed together. The results from this re-analysis are summarised in the chart of Fig. 6d. According to this figure, the fatigue strength of the hybrid welded joints manufactured by employing aluminium alloy AA1050 can be modelled

effectively via a master curve having Mode I N-SIF range at $5 \cdot 10^6$ cycles to failure equal to 25 MPa·mm$^{0.326}$ (for P_s=to 97.7%) and negative inverse slope, k, equal to 3.5.

To conclude, examination of the state of the art certainly demonstrates that the N-SIFs approach is a very powerful tool suitable for estimating the fatigue strength of welded joints by systematically reaching an adequate level of accuracy [69-74]. However, to successfully extend the usage of this design methodology to those situations involving not only very small thicknesses but also very low strength aluminium alloys, a different master curve should be derived by post-processing a large number of appropriate experimental results.

6. Fatigue design according to the MWCM applied along with the Point Method

As defined by Taylor [75], the Theory of Critical Distances (TCD) is a theoretical framework grouping together different methods that all make use of a length scale parameter to estimate fatigue strength in the presence of stress concentrators of all kinds [19, 21]. This material length scale parameter is commonly referred to as the "critical distance".

The TCD can be formalised in different ways, including the Point Method (PM), the Line Method, the Area Method, and the Volume Method [21, 76]. The PM [76] represents the simplest formulation of the TCD and can be used to estimate the fatigue strength of either notched, cracked, or welded structural components. Owing to its simplicity, this formalisation of the TCD will be used to assess the fatigue strength of the aluminium-to-steel hybrid welded joints tested in this experimental series. In particular, the PM will be applied along with the so-called Modified Wöhler Curve Method (MWCM), with the latter design tool being a bi-parametrical critical plane approach suitable for assessing those situations involving multiaxial fatigue loading. This will be done to rigorously assess the damage resulting from the three-dimensional stress fields acting on the material in the vicinity of the weld toes/roots. In real welded structures, the stress states at the critical locations are always multiaxial [39]. Therefore, three-dimensional FE analyses should always be carried out to estimate the spatial distribution of the stress fields of interest, with this resulting in more accurate fatigue assessment. Unfortunately, three-dimensional numerical simulations are very time-consuming because they require the use of a large number of 3D elements to achieve a very fine mesh in the critical regions. However, under some particular circumstances, the complexity of 3D problems can be reduced by solving simpler 2D models. This can be done although, sometimes, simplified 2D analyses result in a loss of accuracy in terms of capability of estimating the actual spatial distribution of the stress fields of interest.

Bearing in mind the issues associated with 3D vs. 2D FE solutions, in what follows, the accuracy of the MWCM/PM in estimating the fatigue lifetime of the aluminium-to-steel welded joints being tested will be checked by post-processing the linear-elastic stress fields determined by solving not only, bi-, but also three-dimensional numerical models.

6.1. Point Method and the Modified Wöhler Curve Method: a brief review

In general terms, to apply the MWCM along with the PM, the critical distance associated with the specific material being designed must be determined by running appropriate experiments [39]. In the TCD framework, for a given material, the critical distance is assumed not to depend on the profile/sharpness of the stress concentrator being designed [75].

As far as welded joints are concerned, this material critical length is used to define, along the weld toe/root bisector, the position of that specific point at which the time-variable design stress state is recommended to be determined. Subsequently, this stress state is post-processed to calculate the stress components relative to that material plane which experiences the maximum shear stress range. Finally, the normal and shear stress components acting on the critical plane are directly used to assess, according to the MWCM, the fatigue lifetime of the welded component being designed. In order to use this methodology in situations of practical interest, Susmel [77, 78] proposed two unifying critical distance values of 0.5 mm and 0.075 mm for steel and aluminium welded joints, respectively. These values for the PM critical distance were derived by re-analysing a large number of experimental data.

The key features of this design approach based on the combined use of the PM and the MWCM will be reviewed in what follows and then extended to the fatigue assessment of steel-to-aluminium welded connections.

The MWCM is a bi-parametric multiaxial fatigue approach which assumes that fatigue damage reaches its maximum value on that material plane experiencing the maximum shear stress range (i.e., the so-called critical plane).

Fig. 7a summarises the procedure based on the PM/MWCM which is recommended as being followed to design welded joints against fatigue [39]. First, multiaxial stress tensor [$\Delta\sigma$] at the critical location must be determined numerically for the specific welded geometry/loading configuration being investigated. As mentioned above, this stress tensor is recommended to be determined at a distance from the crack initiation point of 0.5 mm for steel welded joints and to 0.075 mm for aluminium weldments [77, 78]. Next, stress tensor [$\Delta\sigma$] is post-processed to calculate the shear range, $\Delta\tau$, and the nominal stress range, $\Delta\sigma_n$, relative to the critical plane [80]. The combined effect of $\Delta\tau$ and $\Delta\sigma_n$ is quantified through the stress ratio ρ_w which is defined as follows [39]:

$$\rho_w = \frac{\Delta\sigma_n}{\Delta\tau} \tag{5}$$

As defined, ρ_w is capable of taking into account the degree of multiaxiality and non-proportionality of the assessed load history [39].

In Fig. 7b the maximum shear stress range, $\Delta\tau$, and the number of cycles to failure, N_f, are plotted against each other in a specific log-log plot which is usually referred to as the Modified Wöhler diagram [71]. As per Fig. 7b, the fatigue curves that are obtained when fatigue strength is modelled according to the MWCM fully depend upon stress ratio ρ_w. Each curve can then be defined explicitly and unambiguously via its negative inverse slope, $k_\tau(\rho_w)$, and its endurance limit, $\Delta\tau_{Ref}(\rho_w)$, where the latter stress quantity is extrapolated at a reference number of cycle to failure equal to N_{Ref}. By post-processing a large number of experimental data, it was demonstrated that functions $k_\tau(\rho_w)$ and $\Delta\tau_{Ref}(\rho_w)$ can be expressed effectively by simply using two linear relationships, i.e. [71, 72]:

$$k_t(\rho_w) = \alpha \cdot \rho_w + \beta \tag{6}$$

$$\Delta\tau_{Ref}(\rho_w) = a \cdot \rho_w + b \tag{7}$$

In Eqs (6) and (7) α, β, a and b are fatigue constants to be determined from suitable experimental design curves. In particular, by remembering that under uniaxial fatigue loading ρ_w is invariably equal to unity, whereas under torsional loading this critical plane stress ratio is invariably equal to zero [39], Eqs (6) and (7) can be rewritten directly as [39, 71]:

$$k_t(\rho_w) = (k - k_0) \cdot \rho_w + k_0 \tag{8}$$

$$\Delta\tau_{Ref}(\rho_w) = \left(\frac{\Delta\sigma_A}{2} - \Delta\tau_A\right) \cdot \rho_w + \Delta\tau_A \tag{9}$$

Here, k and k_0 are the negative inverse slopes of the uniaxial and torsional fatigue curves, respectively, and $\Delta\sigma_A$ and $\Delta\tau_A$ are the range of the corresponding endurance limits extrapolated at a number of cycles to failure equal to N_{Ref}.

To conclude, via a systematic validation exercise based on a large number of experimental results, it has been demonstrated that the MWCM is highly accurate in estimating the fatigue strength of both steel and aluminium welded joints when subjected to in-service constant/variable amplitude in-phase/out-of-phase uniaxial/multiaxial fatigue loading [37, 79-87].

6.2. The MWCM applied along with PM to estimate fatigue lifetime of aluminium-to-steel welded connections

In order to use the MWCM in conjunction with the PM to estimate the fatigue lifetime of the aluminium-to-steel thin welded joints that have been tested, the first step is calibration of governing equations (8) and (9) to take into account the actual strength of these hybrid connections. The procedure used to estimate the relevant fatigue constants is described below. Initially, linear-elastic bi-dimensional and tri-dimensional FE models were solved via commercial software ANSYS® (see the examples shown in Figs 5b and 5c). The 3D FE models for the different welded configurations were solved by following a standard solid-to-solid sub-modelling procedure. The mesh density for the 2D and 3D models was increased gradually until convergence occurred (Fig.8a).

For the 2D models, as per the example shown in Fig. 7a (see also the FE model on the left had side in Fig. 8a), the relevant local stress states, $[\Delta\sigma]$, were determined at a distance from the crack initiation point equal to 0.075 mm. For the 3D models, the local stresses were (still) extrapolated, along the bisector, at a distance from the weld toe equal to 0.075 mm and calculated for the entire width of the specimen (Fig. 9). Following the same procedure as the one proposed in Ref. [88] for the static case, the required effective stresses were then determined at a distance equal to 0.075 mm away from the edge of the weld as shown in Fig. 9.

The stress-distance curves plotted in the graphs of Fig. 9 also allow the 3D stress analysis solutions to be compared directly with those obtained by solving simpler 2D FE models. These graphs make it evident that the use of bi-dimensional models resulted in linear-elastic stress distributions with a lower magnitude than the one that was obtained from the corresponding 3D models.

As per Fig. 9, since, as expected, the use of the 2D solutions was seen to result in a lower magnitude of the relevant linear-elastic stresses, the results from the bi-dimensional numerical analyses were then used to calibrate the MWCM's governing equations. By post-processing the relevant stress states determined from bi-dimensional FE models, the normal stress range, $\Delta\sigma_n$, and the shear stress range, $\Delta\tau$, relative to the critical plane were calculated using the methodology formulated and validated in Refs [80, 89] (Fig.8b). The experimental values of the critical plane shear stress ranges, $\Delta\tau$, were then post-processed, for each welded geometry, according to the statistical procedure reviewed in [39] to estimate, at $5 \cdot 10^6$ cycles to failure, the corresponding endurance limit range $\Delta\tau_{A,50\%}$ (for P_s equal to 50%). The endurance limits determined by solving 2D FE models and characterised by the maximum and minimum value of stress ratio ρ_w were then selected to estimate the constants in the $\Delta\tau_{Ref}$ vs. ρ_w relationship, Eq. (7). The function $\Delta\tau_{Ref}(\rho_w)$ was calibrated using the results generated by testing under R=0.1 the butt-welded joint (resulting in ρ_w=3.37) and under R=0.5 the lap-welded joints (resulting in ρ_w=1.73). According to this simple procedure [37, 39], the function

suitable for estimating the reference shear stress range, $\Delta\tau_{Ref}(\rho_w)$, at $5 \cdot 10^6$ cycles to failure was derived as follows for P_s equal to 50% (Fig. 8d):

$$\Delta\tau_{Ref}(\rho_w) = -1.7 \cdot \rho_w + 16.4 \text{ [MPa]} \quad (10)$$

and as follows for P_s equal to 97.7%:

$$\Delta\tau_{Ref}(\rho_w) = -1.2 \cdot \rho_w + 11.4 \text{ [MPa]} \quad (11)$$

The k_τ vs. ρ_w relationship, Eq. (6), was determined using the values for the negative inverse slope that are recommended by Sonsino et al. [47] for thin and flexible welded joints (i.e., k=5 under uniaxial fatigue loading and k_o=7 under torsional fatigue loading). Accordingly, function $k_\tau(\rho_w)$ was assumed to take the following form (Fig. 8d) [37, 39]:

$$k_\tau(\rho_w) = -2 \cdot \rho_w + 7 \quad \text{for } \rho_w \leq 1 \quad (12)$$

$$k_\tau(\rho_w) = 5 \quad \text{for } \rho_w > 1 \quad (13)$$

The modified Wöhler diagrams reported in Figs 10 and 11 summarise the level of accuracy that was obtained by applying the MWCM in conjunction with the PM to estimate the fatigue lifetime of the aluminium-to-steel thin welded joints we tested. The results summarised in Fig. 10 and in Fig. 11 were obtained by post-processing the linear-elastic stress distributions calculated via 2D and 3D FE models, respectively, and by taking the PM critical distance equal to 0.075 mm [77]. As can be seen from the diagrams of Figs 10 and 11, by performing simple, standard linear-elastic FE analysis, the use of the MWCM applied along with the PM results in highly accurate estimates, with this holding true independently of the complexity of the numerical models being solved to determine the required linear-elastic stress fields.

7. Conclusions

Based on using different design techniques, the present paper provides a comprehensive assessment of the fatigue strength of aluminium-to-steel thin welded joints. The key findings from the present investigation are summarised below.

- Except for the tee-welded joints (Fig. 1d), the visual examination of the fracture surfaces in the hybrid welded joints being tested revealed that fatigue cracks initiated at the weld toe on the aluminium side. Therefore, aluminium-to-steel hybrid joints can be designed against fatigue by treating them as conventional aluminium-to-aluminium welded connections.

- As far as the nominal stress approach is concerned, the value of 5 for the negative inverse slope, k, suggested by Sonsino et al. [47] for thin welded connections (i.e., for connections having thickness of the main plate lower then 5 mm) was seen to provide conservative estimates of the fatigue strength of the aluminium-to-steel welded joints being tested.
- A FAT90 design curve is recommended to estimate the fatigue strength of thin hybrid welded joints according to the effective notch stress approach.
- When applying the N-SIF approach, a reference design curve with $\Delta K_{I,97,7\%}$ equal to 25 MPa·mm$^{0.326}$ at $5 \cdot 10^6$ cycles to failure and k equal to 3.5 is suggested to estimate the fatigue life of aluminium-to-steel thin welded joints with a high level of conservatism.
- The MWCM applied along with the PM was seen to be highly accurate in estimating the fatigue lifetime of the thin aluminium-to-steel welded joints being tested, with this holding true independently of the complexity of the numerical stress analysis being performed to determine the relevant linear-elastic stress fields.

Acknowledgements

EWM® (www.ewm-group.com) is acknowledged for supporting the present research investigation.

References

[1] Schijve J. Fatigue predictions of welded joints and the effective notch stress concept. Int J Fatigue 2012; 45:31-38

[2] Haryadi GD, Kim SJ. Influences of post weld heat treatment on fatigue crack growth behavior of TIG welding of 6013 T4 aluminium alloy joint (part 1. Fatigue crack growth across the weld metal). J Mech Sci and Tech 2011; 25(9):2161-2170.

[3] Borrego LP, Costa JD, Jesus JS, Loureiro AR, Ferreira JM. Fatigue life improvement by friction stir processing of 5083 aluminium alloy MIG butt welds. Theor App Fract Mech 2014; 70:67-74.

[4] Fricke W. Review Fatigue analysis of welded joints: state of development. Marine Structures 2003; 16:185-200.

[5] Schijve J. Fatigue of Structures and Materials, Second Edition ed., Springer, 2009.

[6] Hobbacher A. Recommendations For Fatigue Design of Welded Joints and Components. International Institute of Welding, Paris, 2007.

[7] EuroCode 9: Design of aluminium structures- Part 1-3: Structures susceptible to fatigue. 2011.

[8] EuroCode 3: Design of steel structures- Part 1-9: Fatigue. 2005.

[9] Radaj D, Sonsino CM, Fricke W. Fatigue assessment of welded joints by local approaches. Cambridge, UK: Woodhead Publishing ; 2007.

[10] Fricke W, Sonsino CM. Notch stress concepts for the fatigue assessment of welded joints-Background and applications. Int J Fatigue 2012; 34: 2-16.

[11] Morgenstern C, Sonsino CM, Hobbacher A, Sorbo F. Fatigue design of aluminium welded joints by local stress concept with the ficitious notch radius of r_f=1 mm. Int J Fatigue 2006;28:881-890.

[12] Sonsino CM. A consideration of allowable equivalent stresses for fatigue design of welded joints according to the notch stress concept with the reference radii r_{ref} =1.00 and 0.05 mm. Welding World 2009; 53(3/4):R64-75.

[13] Karakas O, Morgenstern C, Sonsino CM. Fatigue design of welded joints from the wrought magnesium alloy AZ31 by the local stress concept with the fictitious notch radii of r_f=1.0 and 0.05 mm. Int J Fatigue 2008; 30: 2210-2219.

[14] Sonsino CM, Hanselka H, Karakas Ö, Gülsöz A, Vogt M, Dilger K. Fatigue design values for welded joints of the wrought magnesium alloy AZ31 (ISO-MgAI3Zn1) according to the nominal, structural and notch stress concepts in comparison to welded steel and aluminium connections. Welding in the World, 2008; 52(5-6):79-94.

[15] Karakas Ö. Consideration of mean-stress effects on fatigue life of welded magnesium joints by the application of the Smith–Watson–Topper and reference radius concepts. Int J Fatigue 2013;49:1-17.

[16] Lazzarin P, Tovo R. A unified approach to the evaluation of linear elastic stress fields in the neighborhood of cracks and notches. Int J Fracture 1996; 78:3-19.

[17] Lazzarin P, Tovo R. A notch intensity factor approach to the stress analysis of welds. Fatigue Fract Engng Mater Struct 1998; 21: 1089-1103.

[18] Williams ML. Stress singularities resulting from various boundary conditions in angular corners of plates in extension. J Appl Mech 1952; 19:526-528.

[19] Taylor D, Barrett N, Lucano G. Some new methods for predicting fatigue in welded joints. Int J Faigue 2002; 24:509-518.

[20] Karakaş Ö, Zhang G, Sonsino CM. Critical distance approach for the fatigue strength assessment of magnesium welded joints in contrast to Neuber's effective stress method. Int J Fatigue 2018;112:21-35.

[21] Crupi G, Crupi V, Guglielmino E, Taylor D. Fatigue assessment of welded joints using critical distance and other methods. Eng Fail Anal 2005; 12:129-142.

[22] Schuber E, Klassen M, Zerner I, Walz C, Sepold G. Light-weight structures produced by laser beam joining for future applications in automobile and aerospace industry. J of Mater Proc Tech 2001; 115(1): 2-8.

[23] Okamura H, Aota K. Joining of dissimilar materials with friction stir welding. Welding International 2004; 18(11): 852-860.

[24] Katayama S. Laser welding of aluminium alloys and dissimilar metals. Welding International 2004; 18(8):618-625.

[25] Kato K, Tokisue H. Dissimilar friction welding of aluminium alloys to other materials. Welding International 2004; 18(11): 861-867.

[26] Lu Z, Huang P, Gao W, Li Y, Zhang H, Yin S. ARC welding method for bonding steel with aluminium. Front. Mech. Eng. China 2009; 4(2):134-143.

[27] Kimapong K, Watanabe T. Lap Joint of A5083 Aluminium Alloy and SS400 Steel by Friction Welding. Mater Trans 2005; 46 (4): 835-841.

[28] Qin GL, Su YH, Wang SJ. Microstructures and properties of welded joint of aluminium alloy to galvanized steel by Nd: YAG laser + MIG arc hybrid brazing-fusion welding. Transactions of Nonferrous Metals Society of China 2004; 24:989-995.

[29] Taban E, Gould J, Lippold J. Dissimilar friction welding of 6061-T6 aluminium and AISI 1018 steel: Properties and microstructural characterization. Mate and desi 2010; 31(5): 2305-2311.

[30] Węglowski M. Friction stir processing technology – new opportunities. Welding International 2013; 28(8): 583-592.

[31] Su Y, Hua X, Wu Y. Effect of input current modes on intermetallic layer and mechanical property of aluminium–steel lap joint obtained by gas metal arc welding. Mate Sci and Eng 2013; 578:340-345.

[32] Xu F, Sun G, Li G. Failure analysis for resistance spot welding in lap-shear specimens. Int J Mech Sci 2014; 78:154-166.

[33] Cao R, Sun JH, Chen JH, Wang P. Cold metal transfer joining aluminum alloys-to-galvanized mild steel. J Manuf Sci Eng 2014; 213(10): 1753-1763.

[34] Goecke S.F. Low Energy Arc Joining Process for Materials Sensitive to Heat. EWM Mündersbach, Germany, 2005.

[35] Al Zamzami I, Di Cocco V, Davison JB, Lacoviello F, Susmel L. Static strength and design of aluminium-to-steel thin welded joints. Welding World 2018; 1-18.

[36] Eurocode 9: Design of aluminium structures – Part 1-1: General structural rules, (1998) prENV.

[37] Susmel L. Four Stress analysos straregies to use the Modified Wöler Curve Method to perform the fatigue assessment of weldments subjected to constant and variable amplitude multiaxial fatigue loading. Int J Fatigue 2014; 64: 38-54.

[38] Djavit D.E, Strande E. Fatigue failure analysis of fillet welded joints used in offshore structures. Master's thesis. Chalmers University of Technology, Goteborg, Sweden, 2013.

[39] Susmel L. Multiaxial notch fatigue- From nominal to local stress/strain quantities, Cambridge: Woodhead Publishing Limited, 2009.

[40] Niemi E. Stress determination for fatigue analysis of welded components. Cambridge, UK: Abington Publishing ; 1995.

[41] Kah P, Suoranta R, Martikainen J. Advanced gas metal arc welding processes. Int J Adv Manuf Technol 2013; 67:655-674.

[42] Elrefaey A, Gouda M, Takahashi M, Ikeuchi K. Characterization of Aluminium/Steel Lap Joint by Friction Stir Welding. J Mate Eng Perf 2005;14(1):12-17.

[43] Liu H, Maeda M, Fujii H, Nogi K. Tensile properties and fracture locations of friction-stir welded joints of 1050-H24 aluminum alloy. J Mate Sci Letters 2003;22:41-43.

[44] Meco S, Pardal G, Ganguly S, Williams S, McPherson N. Application of laser in seam welding of dissimilar steel to aluminium joints for thick structural components. Optics and Laser in Engineering 2015: 22-30.

[45] Katayama S. Laser welding of aluminium alloys and dissimilar metals. Welding International 2004; 18(8): 618-625.

[46] Wang P, Chen X , Pan Q, Madigan B, Long J. Laser welding dissimilar materials of aluminum to steel: an overview. Int J Adv Manuf Tech 2016;87:3081-3090.

[47] Sonsino C. M, Bruder T, Baumgartner J, "S-N Lines for welded thin joints- suggested slopes and FAT values for applying the notch stress concept with various reference radii. Welding World 2010; 54(11/12): R375-392.

[48] Fricke W. Round-Robin study on stress analysis for the effective notch stress approach. Welding World 2007; 51(3/4): 68-79.

[49] Radaj D. Design and analysis of fatigue resistant welded structures, Cambridge, England: Abington Publishing, 1990.

[50] Berto F, Lazzarin P, Radaj D. Fictitious notch rounding concept applied to V-notches with root hole subjected to in-plane mixed mode loading. Eng Fract Mech 2014; 128:171-188.

[51] Radaj D, Lazzarin P, Berto F. Generalised Neuber concept of fictitious notch rounding. Int J Fatigue 2013;51:105-115.

[52] Berto F, Lazzarin P, Radaj D. Fictitious notch rounding concept applied to V-notches with root holes sibjected to in-plane shear loading. Eng Fract Mech 2012; 79:281-294.

[53] Berto F, Lazzarin P, Radaj D. Application of the fictitious notch rounding approach to notches with end-holes under mode 2 loading. SDHM Structural Durability and Health Monitoring 2012; 8(1):31-44.

[54] Creager M, Paris P.C. Elastic field equations for blunt cracks with reference to stress corrosion cracking. Int J Fracture Mechanics 1967; 3:247-252.

[55] Fricke W. IIW guideline for the assessment of weld root fatigue. Welding World 2013;57:753-791.

[56] Morgenstern C. Fatigue design of aluminium welded joints by the local stress concept with the fictitious notch radius of r_f=1mm. Int J Fatigue 2006; 28:881-890.

[57] Karakaş Ö. Application of neuber's effective stress method for the evaluation of the fatigue behaviour of magnesium welds. Int J Fatigue 2017; 101:115-126.

[58] Verreman Y, Nie B. Early development of fatigue cracking at manual fillet welds. Fatigue Fract Engng Mater Struct 1996; 19(6):669-681.

[59] Radaj D. State-of-the-art review on the local strain energy density concept and its relation to the J-integral and peak stress method. Fatigue Fract Eng Mater Struct 2015;38(1):2-28.

[60] Radaj D. State-of-the-art review on extended stress intensity factor concepts. Fatigue Fract Eng Mater Struct 2014; 37(1);1-28.

[61] Lazzarin P, Lassen T, Livieri P. A notch stress intensity approach applied to fatigue life predictions of welded joints with different local toe geometry. Fatigue Fract Engng Mater Struct 2003; 26:49-58.

[62] Lazzarin P, Tovo R. A unified approach to the evaluation of linear elastic stress fields in the neighborhood of cracks and notches. Int J Fracture 1996; 78:3-19.

[63] Atzori B, Lazzarin P, Tovo R. Stress field parameters to predict the fatigue strength of notched components. J Str Anal 1999; 34(6):437-453.

[64] Lazzarin P, Tovo R. A notch Intensity Factor Approach to the Stress Analysis of Welds. Fatigue & Fract of Eng Mate & Struct 1998; 21:1089-1103.

[65] Tovo R, Lazzarin P. Relationships between local and structural stress in the evaluation of the weld toe stress distribution. Int J Fatigue 1999;21:1063-1078.

[66] Lazzarin P, Livieri P. Notch stress intensity factors and fatigue strength of aluminium and steel welded joints. Int J Fatigue 2001; 23:225-232.

[67] Maddox SJ. Effect of plate thickness on the fatigue strength of fillet welded joints. Abington, Cambridge: Abington Publishing, 1987.

[68] Gurney TR. The Fatigue strength of transverse fillet welded joints: a study of the influence of the joint geometry. Cambridge: Abington Publishing, 1991.

[69] Fischer C, Fricke W, Rizzo C.M. Review of the fatigue strength of welded joints based on the notch stress intensity factor and SED approaches. Int J Fatigue 2016; 84:59-66.

[70] Atzori B, Lazzarin P, Meneghetti G, Ricotta M. Fatigue design of complex welded structures. Int J Fatigue 2009; 31:59-69.

[71] Susmel L, Lazzarin P. A bi-parametric modified Wöhler curve for high cycle multiaxial fatigue assessment. Fatigue Fract Engng Mater Struct 2002;25:63-78.

[72] Susmel L, Tovo R. Local and structural multiaxial stress states in welded joints under fatigue loading. Int J Fatigue 2006; 28:564-575.

[73] Susmel L. Estimating fatigue lifetime of steel weldments locally damaged by variable amplitude multiaxial stress fields. Int J Fatigue 2010; 32:1057-1080.

[74] Al Zamzami I, Susmel L. On the accuracy of nominal, structural, and local stress based approaches in designing aluminium welded joints against fatigue. Int J Fatigue 2017; 101:137-158.

[75] Taylor D. The theory of critical distances- a new perspective in fracture mechanics, Oxford, UK: Elsevier, 2007.

[76] Taylor D. Geometrical effects in fatigue: a unifying theoretical model. Int J Fatigue 1999; 21(5): 413-420.

[77] Susmel L. The Modified Wöhler Curve Method calibrated by using standard fatigue curves and applied in conjunction with the Theory of critical distances to estimate fatigue lifetime of aluminium weldments. Int J Fatigue 2009; 31:197-212.

[78] Susmel L. Modified Wöhler Curve Method, Theory of Critical Distances and EUROCODE 3: a novel engineering procedure to predict the lifetime of steel welded

joints subjected to both uniaxial and multiaxial fatigue loading. Int J Fatigue 2008; 30:888-907.

[79] Susmel L, Tovo R. On the use of nominal stresses to predict the fatigue strength of welded joints under biaxial cyclic loading. Fatigue Fract Eng Mater Struct 2004; 27:1008-1024.

[80] Susmel L. A simple and efficient numerical algorithm to determine the orientation of the critical plane in multiaxial fatigue problems. Int J Fatigue 2010;32:1875–1883.

[81] Susmel L, Tovo R. Local and structural multiaxial stress states in welded joints under fatigue loading. Int J Fatigue 2006; 28:564-575.

[82] Susmel L, Tovo R, Benasciutti D. A novel engineering method based on the critical plane concept to estimate the lifetime of weldments subjected to variable amplitude multiaxial fatigue loading. Fatigue Fract Eng Mater Struct 2009; 32:441-459.

[83] Susmel L. Three different ways of using the Modified Wöhler Curve Method to perform the multiaxial fatigue assessment of steel and aluminium welded joints. Eng Fail Anal 2009; 16:1074-1089.

[84] Susmel L. Estimating fatigue lifetime of steel weldments locally damaged by variable amplitude multiaxial stress fields. Int J Fatigue 2010; 32:1057-1080.

[85] Susmel L, Sonsino CM, Tovo R. Accuracy of the Modified Wöhler Curve Method applied along with the r_{ref}=1 mm concept in estimating lifetime of welded joints subjected to multiaxial fatigue loading. Int J Fatigue 2011;33:1075-1091.

[86] Susmel L, Harm A. Modified Wöhler Curve Method and multiaxial fatigue assessment of thin welded joints. Int J Fatigue 2012; 43:30-42.

[87] Al Zamzami I, Susmel L. On the use of hot-spot stresses, effective notch stresses and the Point Method to estimate lifetime of inclined welds subjected to uniaxial fatigue loading. Int J Fatigue 2018; 117:432-449.

[88] Ameri AAH, Davison, JB, Susmel L. On the use of linear-elastic local stresses to design load-carrying fillet-welded steel joints against static loading. Eng Frac Mec 2015; 136:38–57.

[89] Susmel L, Tovo R, Socie DF. Estimating the orientation of Stage I crack paths through the direction of maximum variance of the resolved shear stress. Int J Fatigue Volume 2014; 58:94-101.

List of Captions

Table 1. Mass chemical composition of the used materials by weight percentage.

Table 2. Fatigue results generated by testing butt welded joints (Fig.1a) statically re-analysed in terms of nominal, effective notch and the N-SIF approaches.

Table 3. Fatigue results generated by testing cruciform welded joints (Fig.1b) statically re-analysed in terms of nominal, effective notch and the N-SIF approaches.

Table 4. Fatigue results generated by testing lap welded joints (Fig.2a) statically re-analysed in terms of nominal, effective notch and the N-SIF approaches.

Table 5. Fatigue results generated by testing tee welded joints (Fig.2b) statically re-analysed in terms of nominal, effective notch and the N-SIF approaches.

Table 6. Summary of the statistical re-analyses for the different approaches/welded geometries

Figure 1. Geometry of the investigate aluminium-to-steel welded joints, butt-welded joints (a); and the load carrying cruciform welded joints (b); lap-welded hybrid welded joints (c); and the tee welded joints (d).

Figure 2. Fatigue Failure of butt, lap and cruciform welded joins.

Figure 3. Accuracy of the nominal stress approach to estimate the fatigue strength of the thin hybrid welded joints.

Figure 4. Weld toe and root rounded according to the reference radius concept (a); FE model for the tee welded joints (b); accuracy of the effective notch stress approach to estimate the fatigue strength of the thin hybrid welded joints (c); results generated for the whole data and FAT90 design curve (d).

Figure 5. Examples of linear elastic FE models (a) and (b) solved using a 2-dimentional models (c) solved using a 3-dimentional models following the standard solid-solid sub-modelling procedure.

Figure 6. Figure 6. Local stress state in the vicinity of the weld toe (a, b); accuracy of the N-SIF approach to estimate the fatigue strength of the thin hybrid welded joints (c); statistical reanalysis for the whole data and proposed design curve (d).

Figure 7. The MWCM to estimate fatigue lifetime of hybrid welded components applied in terms Point Method (a); Modified Wöhler diagram (b).

Figure 8. The procedure used to calibrate the MWCM constants and estimate the fatigue strength of hybrid welded joint according to the PM.

Figure 9. 2D and 3D linear elastic stress distribution along the weld seam for the cruciform welded joints.

Figure 10. Accuracy of the MWCM applied along with the Point Method in estimating fatigue strength of thin hybrid welded components (2D FE models).

Figure 11. Accuracy of the MWCM applied along with the Point Method in estimating fatigue strength of thin hybrid welded components (3D FE models).

Tables

Table 1. Mass chemical composition of the used materials by weight percentage.

Alloy	Chemical composition [weight%]							
AA1050	Cu	Mg	Si	Fe	Mn	Zn	Ti	Al
	0-0.05	0-0.05	0.25	0-0.4	0.05	0.07	0-0.05	Balanced
EN10130:199	C	P	S	Mn	Fe			
	0.12	0.045	0.045	0.60	Balanced			
AA4043	Cu	Mg	Si	Fe	Mn	Zn	Ti	Al
	0.01	0.05	4.5-6.0	0.80	0.05	0.1	0.2	Balanced

Table 2. Fatigue results generated by testing butt welded joints (Fig.1a) statically re-analysed in terms of nominal stress and effective notch stress approaches.

Code	R	t	W	a	$\Delta\sigma_{nom}$	$\Delta\sigma_{eff}$	N_f	Run Out
		[mm]	[mm]	[mm]	[MPa]	[MPa]	[Cycles to failure]	
Butt_0.1_1	0.1	0.99	49.00	1.88	60	420	15617	
Butt_0.1_2	0.1	1.10	49.80	1.60	50	350	2000000	●
Butt_0.1_3	0.1	1.00	50.80	1.89	54	378	289490	
Butt_0.1_4	0.1	1.02	49.92	2.10	57	399	89952	
Butt_0.1_5	0.1	1.03	50.05	2.17	57	399	105241	
Butt_0.1_6	0.1	1.01	49.73	2.14	54	378	14380	
Butt_0.1_7	0.1	1.01	50.43	1.92	52	364	23470	
Butt_0.1_8	0.1	1.03	49.85	1.66	50	350	23335	
Butt_0.1_9	0.1	1.01	50.34	1.82	50	350	138007	
Butt_0.1_10	0.1	1.02	49.97	1.96	60	420	15275	
Butt_0.1_11	0.1	1.04	50.67	1.78	50	350	67660	
Butt_0.1_12	0.1	1.03	49.84	1.88	50	350	36631	
Butt_0.1_13	0.1	1.03	49.50	1.97	35	245	837329	
Butt_0.1_14	0.1	1.00	49.41	2.10	40	280	2000000	●
Butt_0.1_15	0.1	1.01	49.84	1.88	45	315	967279	
Butt_-1_1	-1	1.96	49.21	2.21	35	525	235783	
Butt_-1_2	-1	1.96	49.12	1.92	42	630	2327	
Butt_-1_3	-1	1.95	49.07	1.79	32	480	138731	
Butt_-1_4	-1	1.97	49.27	2.01	35	525	6415	
Butt_-1_5	-1	1.97	49.32	2.13	30	450	162306	
Butt_-1_6	-1	1.98	50.41	1.87	28	420	2000000	●
Butt_-1_7	-1	1.98	50.41	1.83	40	600	25032	
Butt_-1_8	-1	1.96	50.45	1.83	32	480	2000000	●
Butt_-1_9	-1	1.96	49.21	1.68	35	525	54914	
Butt_-1_10	-1	1.99	50.24	2.00	28	420	2000000	●
Butt_-1_11	-1	1.99	50.24	2.13	38	570	9857	
Butt_-1_12	-1	1.98	50.25	2.09	28	420	41366	

Table 3. Fatigue results generated by testing cruciform welded joints (Fig.1b) statically re-analysed in terms of nominal, effective notch and the N-SIF approaches.

Code	R	t	w	Z1	Z2	L1	$\Delta\sigma_{nom}$	$\Delta\sigma_{eff}$	ΔK_I	N_f	Run Out
		[mm]	[mm]	[mm]	[mm]	[mm]	[mm]	[MPa]	[MPa·mm$^{0.326}$]	[Cycles to failure]	
Cr_0.1_1	0.1	1.02	49.83	5.07	7.43	25.07	60	256	103	1656	
Cr_0.1_2	0.1	1.02	50.73	5.27	7.84	25.27	55	235	95	52093	
Cr _0.1_3	0.1	1.02	49.73	5.21	7.67	25.21	50	214	86	51492	
Cr _0.1_4	0.1	1.03	49.78	4.66	7.51	24.66	50	214	86	327683	
Cr _0.1_5	0.1	1.04	48.98	5.13	7.33	25.13	60	256	103	21171	
Cr _0.1_6	0.1	1.01	48.56	5.18	7.62	25.18	55	235	95	564736	
Cr _0.1_7	0.1	1.02	50.62	5.56	8.10	25.56	40	171	69	564974	
Cr _0.1_8	0.1	1.01	50.60	5.23	7.20	25.23	40	171	69	279615	
Cr _0.1_9	0.1	1.01	50.58	5.49	7.95	25.49	45	192	78	86145	
Cr _0.1_10	0.1	1.01	50.49	5.66	7.58	25.66	45	192	78	2456047	
Cr _-1_1	-1	1.97	48.19	4.04	4.65	24.04	60	256	120	44535	
Cr _-1_2	-1	1.97	48.49	3.97	5.14	23.97	60	256	120	122917	
Cr _-1_3	-1	1.98	48.09	4.30	4.96	24.3	55	235	110	289083	
Cr _-1_4	-1	1.99	47.63	3.77	4.62	23.77	55	235	110	220433	
Cr _-1_5	-1	1.97	48.27	2.89	5.38	22.89	50	214	100	417151	
Cr _-1_6	-1	1.99	48.39	3.58	4.75	23.58	50	214	100	242154	
Cr _-1_7	-1	1.99	47.70	3.84	4.96	23.84	45	192	90	2000000	•
Cr _-1_8	-1	1.99	47.70	3.25	5.07	23.25	55	235	110	297435	
Cr_-1_9	-1	1.99	48.16	3.66	4.95	23.66	48	205	96	188002	
Cr_-1_10	-1	1.98	48.76	3.68	4.50	23.68	48	205	96	699617	
Cr _-1_11	-1	1.98	48.10	3.33	5.55	23.33	48	205	96	2000000	•
Cr _-1_12	-1	1.98	48.10	3.33	5.55	23.33	58	248	116	89987	

Table 4. Fatigue results generated by testing lap welded joints (Fig.2a) statically re-analysed in terms of nominal, effective notch and the N-SIF approaches.

Code	R	t	w	Z1	Z2	L1	L2	$\Delta\sigma_{nom}$	$\Delta\sigma_{eff}$	ΔK_I	N_f	Run Out
		[mm]	[mm]	[mm]	[mm]	[mm]	[mm]	[MPa]	[MPa]	[MPa·mm$^{0.32}$]	[Cycles to failure]	
Lap_0.1_1	0.1	1.02	50.11	2.92	2.83	22.92	22.83	60	234	96	31581	
Lap_0.1_2	0.1	1.01	50.21	3.03	3.15	23.03	23.15	60	234	96	102426	
Lap_0.1_3	0.1	1.01	50.20	2.42	2.37	22.42	22.37	65	253	104	94739	
Lap_0.1_4	0.1	1.03	50.14	2.73	2.44	22.73	22.44	65	253	104	55703	
Lap_0.1_5	0.1	1.01	50.09	2.53	2.63	22.53	22.63	55	214	88	86888	
Lap_0.1_6	0.1	1.02	50.29	3.02	2.80	23.02	22.8	55	214	88	94390	
Lap_0.1_7	0.1	0.98	50.17	2.79	2.55	22.79	22.55	50	195	80	367625	
Lap_0.1_8	0.1	1.00	50.28	2.61	2.97	22.61	22.97	45	175	72	191873	
Lap_0.1_9	0.1	1.01	50.17	2.53	2.64	22.53	22.64	45	175	72	1131920	
Lap_0.1_10	0.1	1.00	50.10	2.66	2.70	22.66	22.7	50	195	80	496799	
Lap_0.5_1	0.5	1.98	51.73	4.89	5.15	24.89	25.15	30	147	67	1093169	
Lap_0.5_2	0.5	1.97	50.34	4.36	5.46	24.36	25.46	35	172	79	275251	
Lap_0.5_3	0.5	1.98	51.82	4.58	5.60	24.58	25.6	35	172	79	209757	
Lap_0.5_4	0.5	1.97	51.75	4.11	6.28	24.11	26.28	30	147	67	929710	
Lap_0.5_5	0.5	1.97	51.73	6.13	4.10	26.13	24.1	32	157	72	467257	
Lap_0.5_6	0.5	1.98	50.48	5.40	3.98	25.4	23.98	32	157	72	531450	
Lap_0.5_7	0.5	1.97	51.76	6.27	4.83	26.27	24.83	28	137	63	2000000	•
Lap_0.5_8	0.5	1.97	50.50	5.04	4.35	25.04	24.35	38	186	85	247044	
Lap_0.5_9	0.5	1.97	51.57	4.14	4.99	24.14	24.99	38	186	85	253922	
Lap_0.5_10	0.5	1.98	50.32	4.81	5.91	24.81	25.91	28	137	63	1037289	

Table 5. Fatigue results generated by testing tee welded joints (Fig.2b) statically re-analysed in terms of nominal, effective notch and the N-SIF approaches.

Code	R	t	t1	w	Z1	Z2	L	$\Delta\sigma_{nom}$	N_f	Run Out
		[mm]	[mm]	[mm]	[mm]	[mm]	[mm]	[mm]	[cycles to failure]	
Tee_0.1_1	0.1	0.99	1.94	50.14	5.75	9.26	25.75	200	634101	
Tee_0.1_2	0.1	1.01	1.93	50.14	5.66	8.85	25.66	200	357228	
Tee_0.1_3	0.1	1.00	1.94	49.97	5.75	8.42	25.75	180	1001833	
Tee_0.1_4	0.1	0.98	1.95	49.88	5.24	7.85	25.24	180	1074989	
Tee_0.1_5	0.1	1.00	1.92	49.66	6.09	8.77	26.09	210	545593	
Tee_0.1_6	0.1	0.98	1.92	50.13	5.15	7.51	25.15	210	2000000	•
Tee_0.1_7	0.1	1.00	1.92	50.13	5.15	7.51	25.15	240	731154	
Tee_0.1_8	0.1	1.00	1.94	50.13	5.72	8.25	25.72	220	429920	
Tee_0.1_9	0.1	0.98	1.94	49.70	5.57	8.89	25.57	220	534240	
Tee_0.1_10	0.1	1.00	1.95	49.99	5.25	8.54	25.25	230	348954	
Tee_0.1_11	0.1	1.02	1.94	49.77	5.77	8.04	25.77	230	269310	
Tee_0.1_12	0.1	1.08	1.93	49.58	5.67	8.02	25.67	210	419127	
Tee_-1_1	-1	1.03	1.96	50.01	5.47	8.11	25.47	220	498691	
Tee_-1_2	-1	1.04	1.96	49.89	5.67	9.33	25.67	220	562767	
Tee_-1_3	-1	1.01	1.96	50.21	5.51	8.52	25.51	210	426377	
Tee_-1_4	-1	1.06	1.95	50.13	5.75	8.42	25.75	190	994315	
Tee_-1_5	-1	1.08	1.95	49.90	5.81	7.41	25.81	200	1074229	
Tee_-1_6	-1	1.02	1.97	49.98	6.02	8.43	26.02	190	1651181	
Tee_-1_7	-1	1.08	1.95	50.01	5.09	7.54	25.09	240	260375	
Tee_-1_8	-1	1.00	1.96	49.98	5.18	8.66	25.18	240	257386	
Tee_-1_9	-1	1.03	1.95	50.27	5.83	7.94	25.83	230	847412	
Tee_-1_10	-1	1.02	1.95	48.67	5.79	8.15	25.79	230	400377	
Tee_-1_11	-1	1.01	1.97	50.00	5.60	8.52	25.60	210	694024	

Table 6 Summary of the statistical re-analyses for the different approaches/welded geometries

Series	No. of Data	R	t	a	Z	k	T_σ	Nominal Stress		Effective Notch Stress		N-SIF Approach	
								$\Delta\sigma_{A,50\%}$	$\Delta\sigma_{A,97.7\%}$	$\Delta\sigma_{A,50\%}$	$\Delta\sigma_{A,97.7\%}$	$\Delta K_{I,50\%}$	$\Delta K_{I,97.7\%}$
			[mm]	[mm]	[mm]			[MPa]	[MPa]	[MPa]	[MPa]	[MPa·mm$^{0.326}$]	[MPa·mm$^{0.326}$]
Butt-joint	12	-1	1.97	1.96	-	7.5	3.4	20.1	10.9	301.7	164.0	-	-
	15	0.1	1.02	1.92	-	7.0	2.8	31.9	19.3	223.4	134.8	-	-
Cruciform-joint	10	-1	1.98	-	3.66	6.8	1.7	38.4	29.3	164.5	125.4	76.9	58.5
	12	0.1	1.02	-	5.25	9.0	3.4	36.2	19.5	154.6	83.2	62.4	33.6
Lap-joint	10	0.1	1.01	-	2.72	6.3	2.1	36.2	24.9	140.6	96.5	57.8	39.8
	10	0.5	1.97	-	4.97	5.8	1.3	25.5	21.7	125.0	107.0	57.3	48.8
Tee-joint	11	-1	1.96	-	5.61	2.9	2.3	132.4	87.9	-	-	-	-
	12	0.1	1.94	-	5.56	5.9	1.5	175.6	145.7	-	-	-	-

Figures

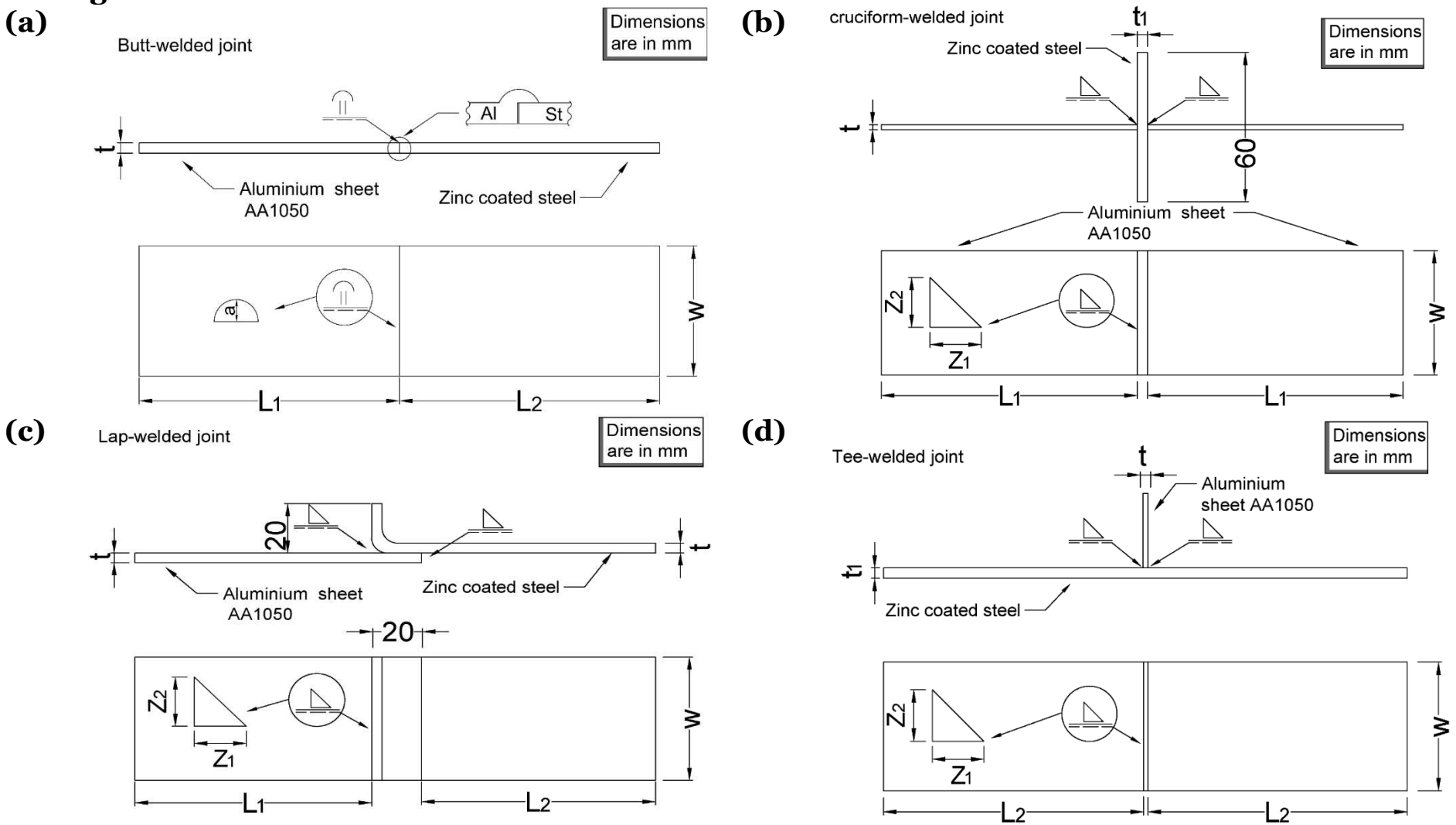

Figure 1. Geometry of the investigated aluminium-to-steel welded joints, butt-welded joints (a); and the load carrying cruciform welded joints (b); lap-welded hybrid welded joints (c); and the tee welded joints (d).

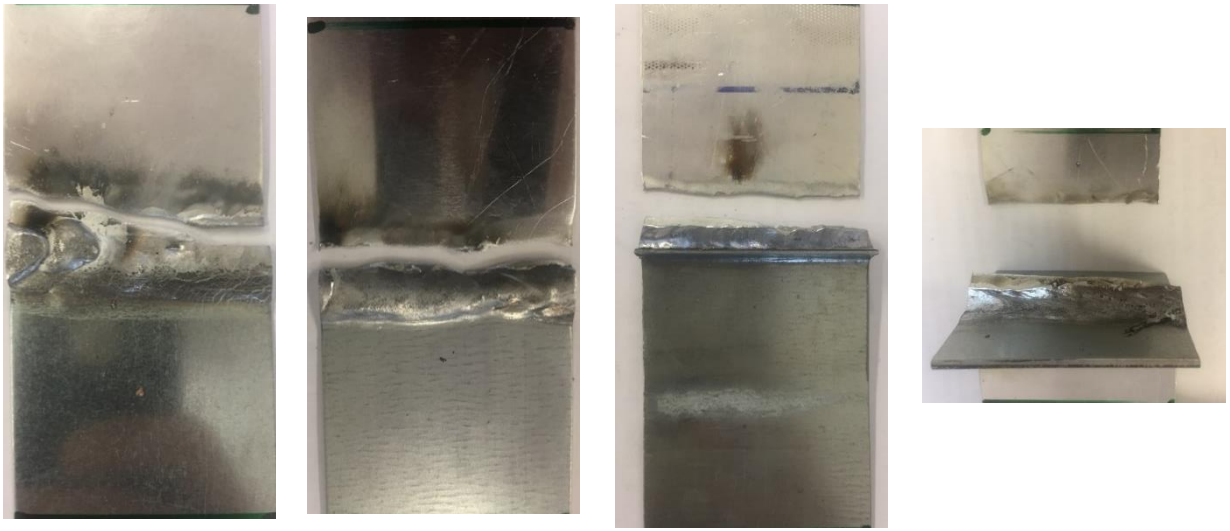

Figure 2. Fatigue Failure of butt, lap and cruciform welded joins.

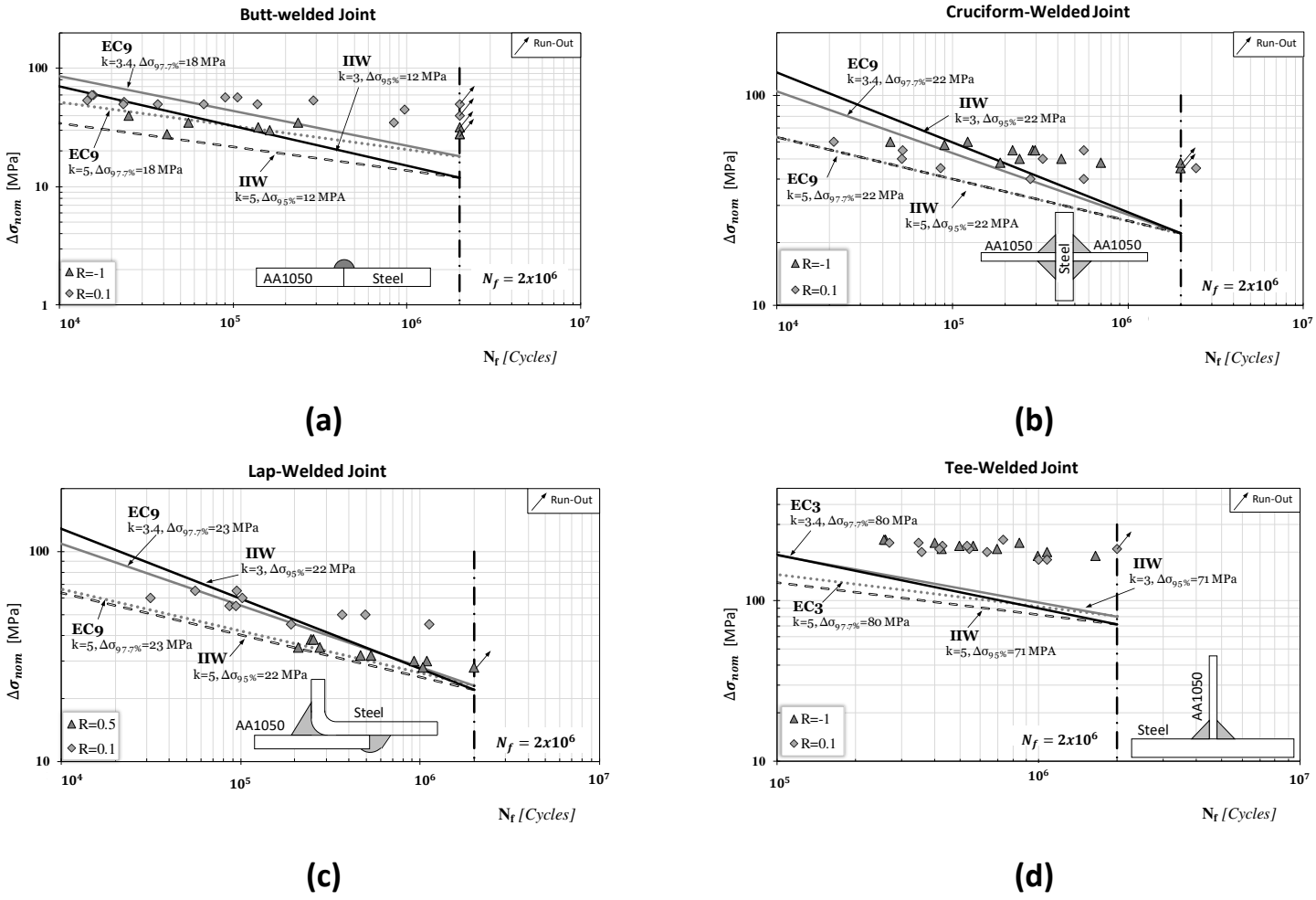

Figure 3. Accuracy of the nominal stress approach to estimate the fatigue strength of the thin hybrid welded joints.

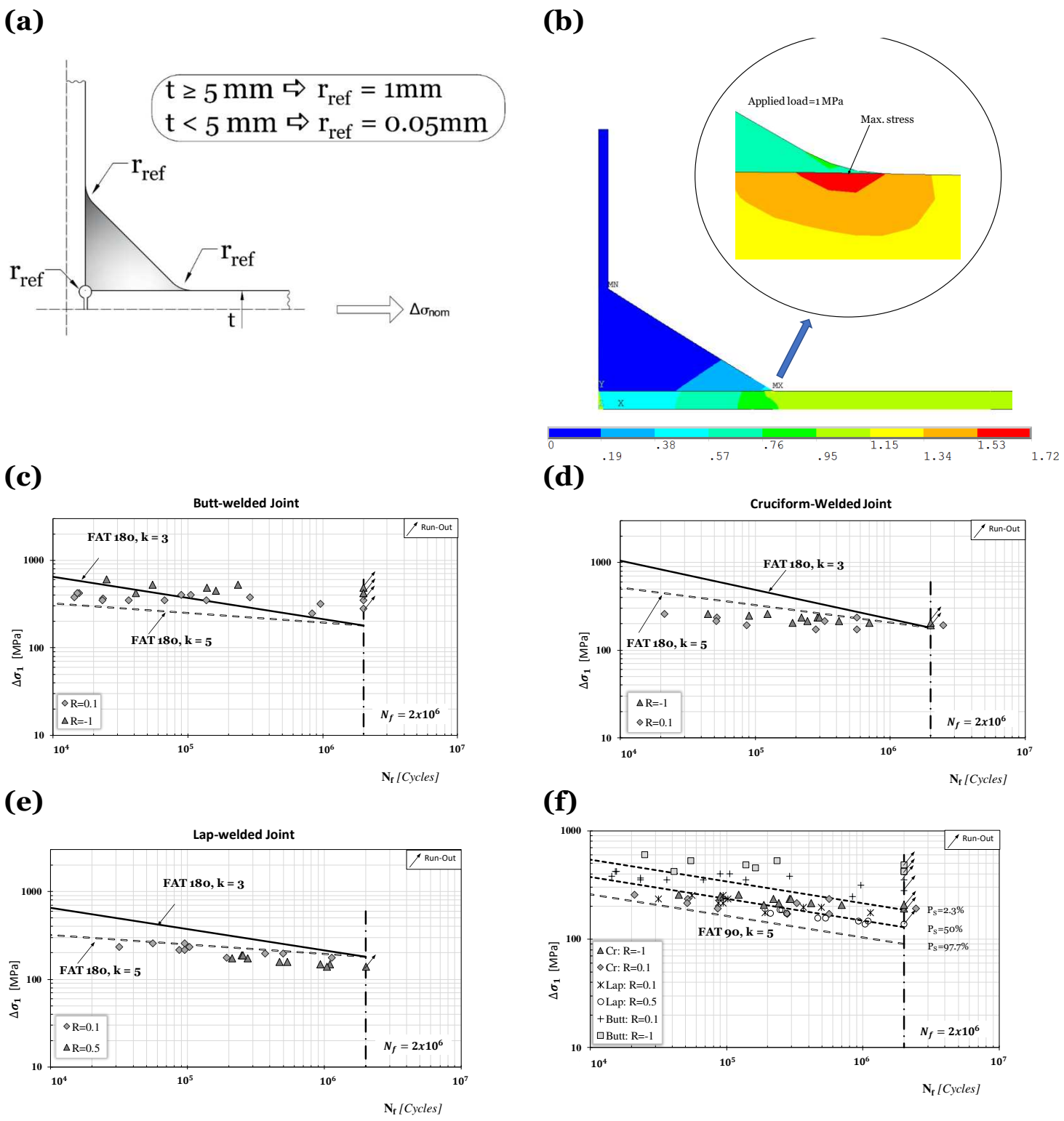

Figure 4. Weld toe and root rounded according to the reference radius concept (a); FE model for the tee welded joints (b); accuracy of the effective notch stress approach to estimate the fatigue strength of the thin hybrid welded joints (c, d, e); results generated for the whole data and FAT90 design curve (f).

(a) 2D Effective notch stress FE models

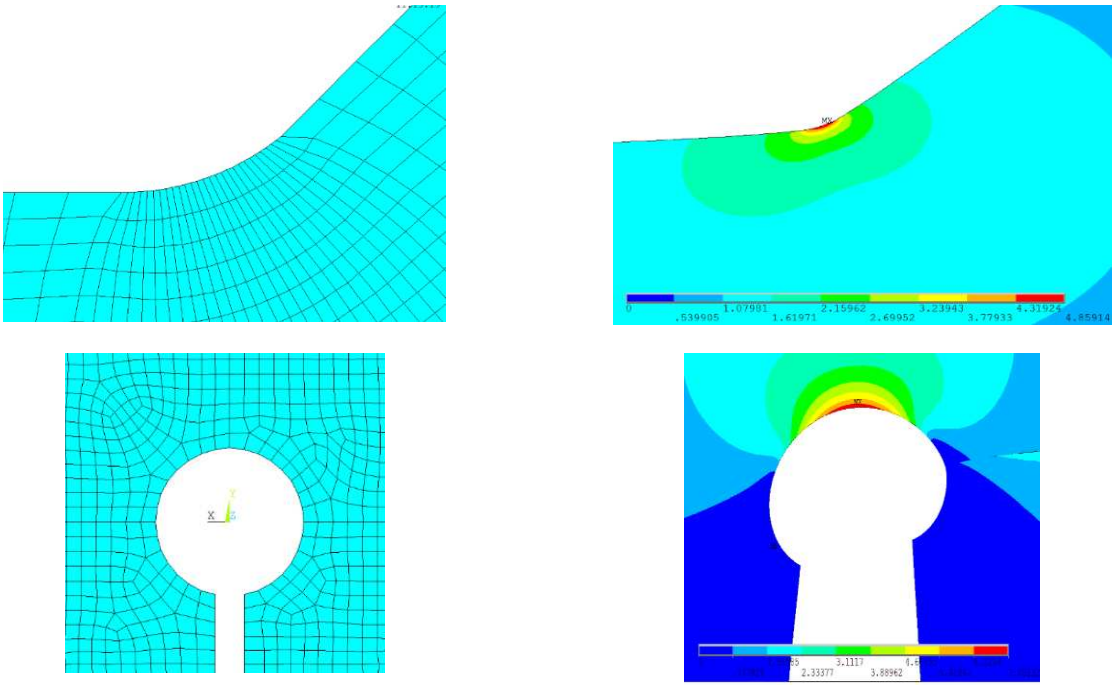

(b) 2D TCD and N-SIF FE models

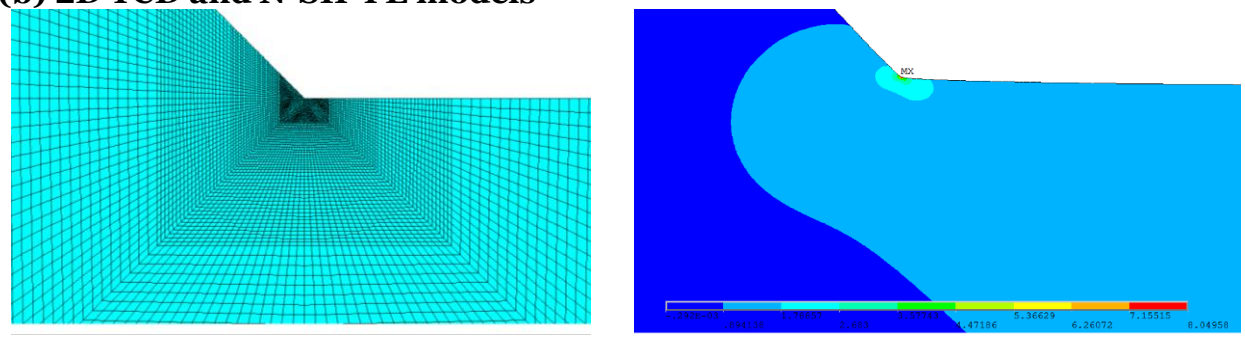

(c) 3D TCD FE Complete model **Sub-model**

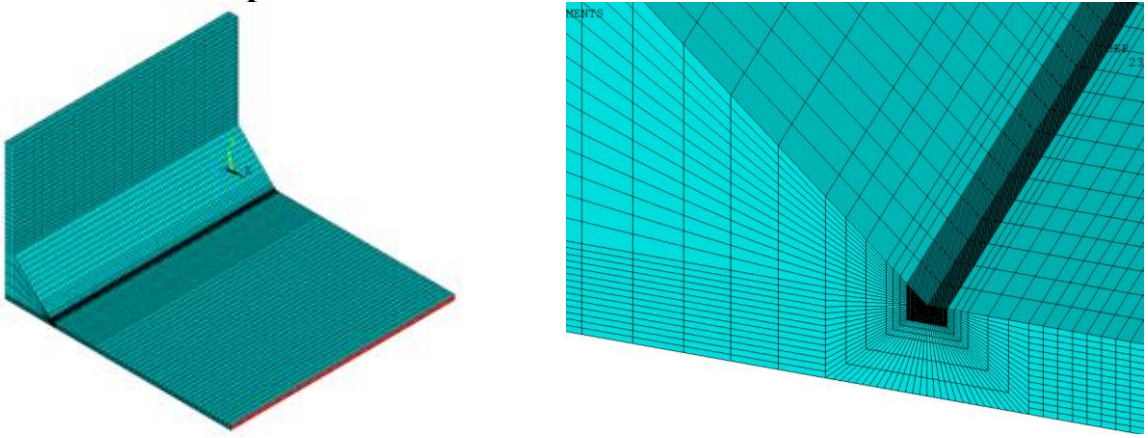

Figure 5. Examples of linear elastic FE models (a) and (b) solved using a 2-dimentional models (c) solved using a 3-dimentional models following the standard solid-solid sub-modelling procedure.

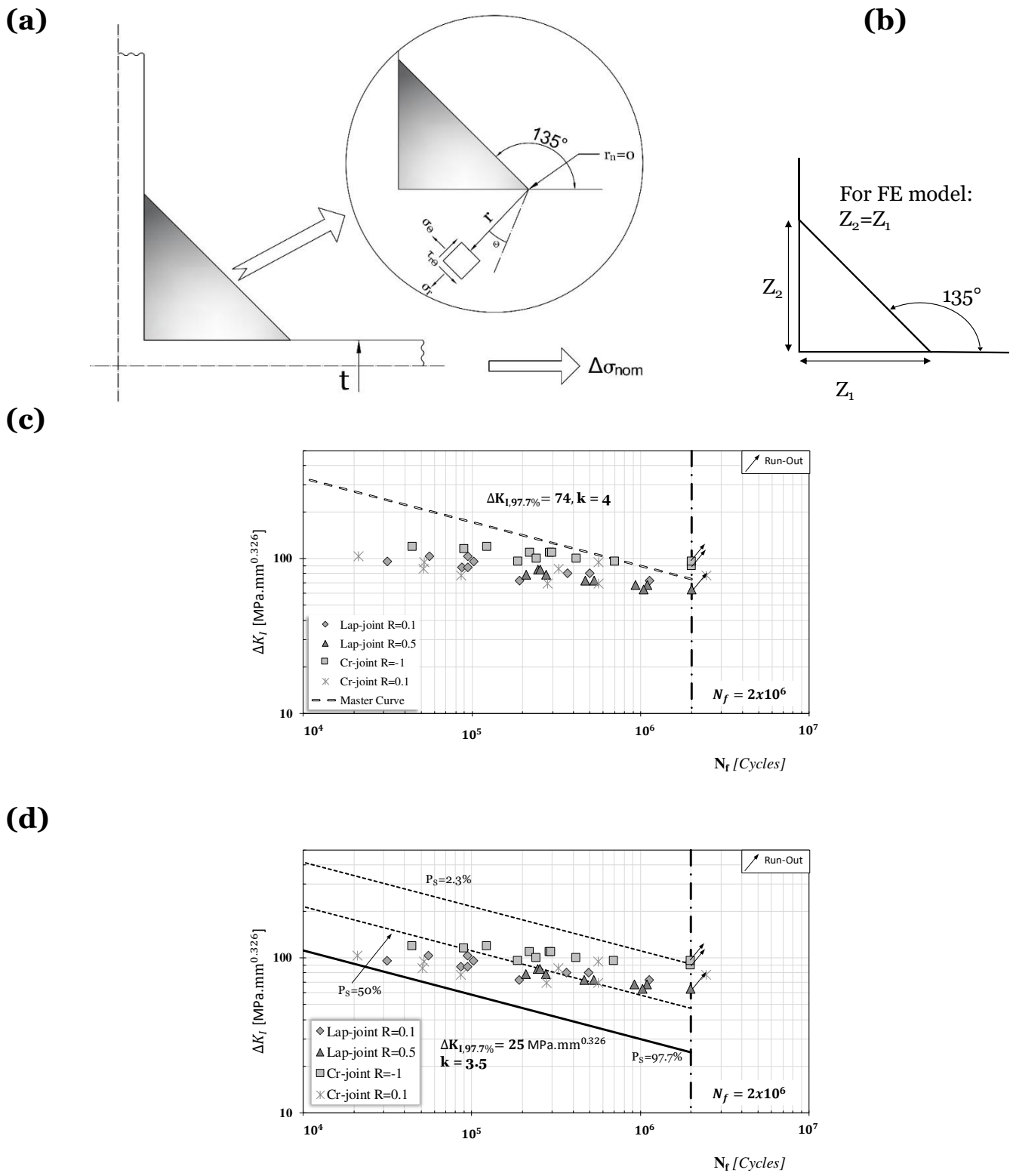

Figure 6. Local stress state in the vicinity of the weld toe (a, b); accuracy of the N-SIF approach to estimate the fatigue strength of the thin hybrid welded joints (c); statistical reanalysis for the whole data and proposed design curve (d).

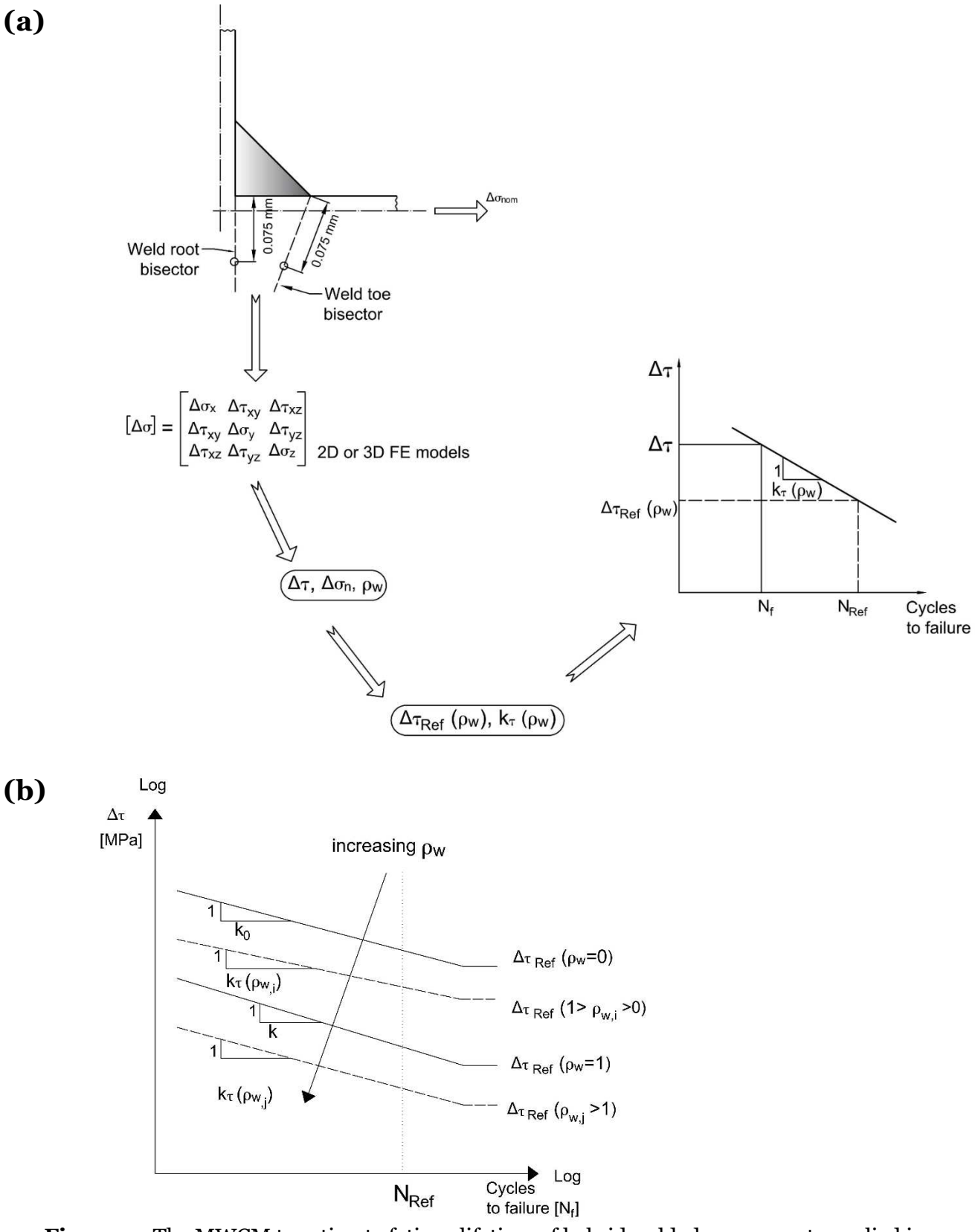

Figure 7. The MWCM to estimate fatigue lifetime of hybrid welded components applied in terms Point Method (a); Modified Wöhler diagram (b)

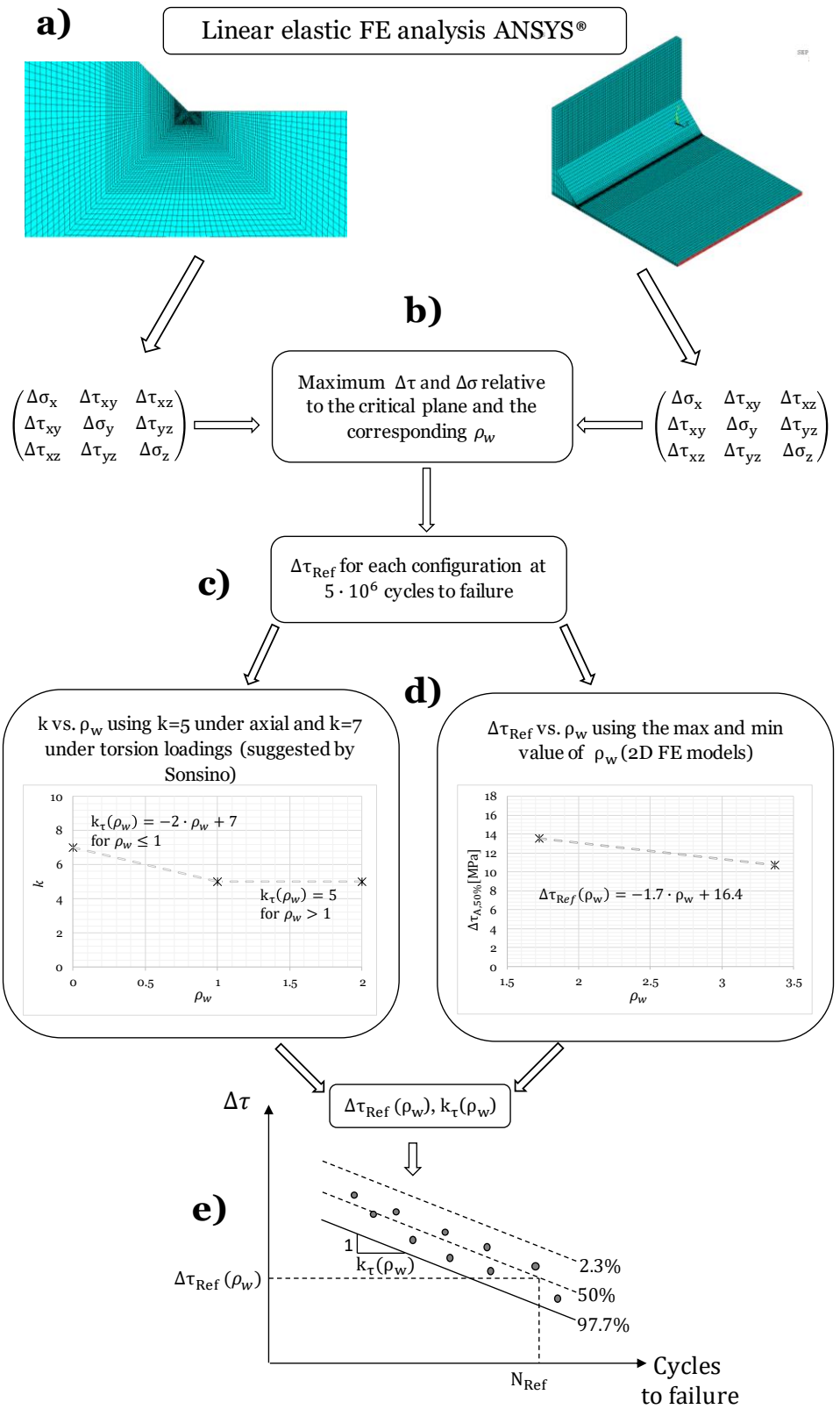

Figure 8. The procedure used to calibrate the MWCM constants and estimate the fatigue strength of hybrid welded joint according to the PM.

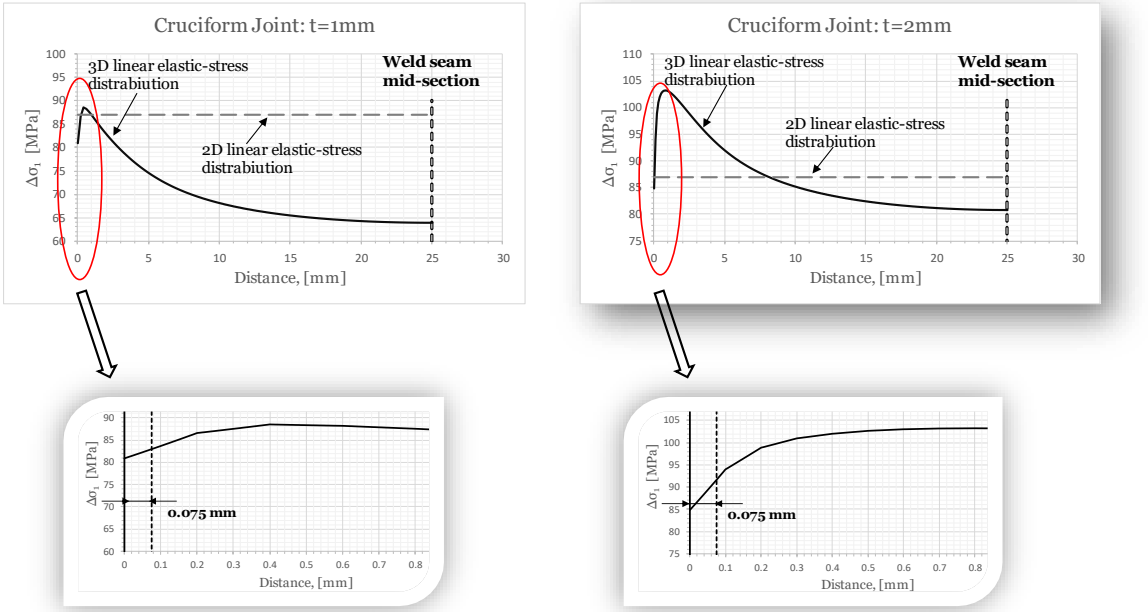

Figure 9. 2D and 3D linear elastic stress distribution along the weld seam for the cruciform welded joints.

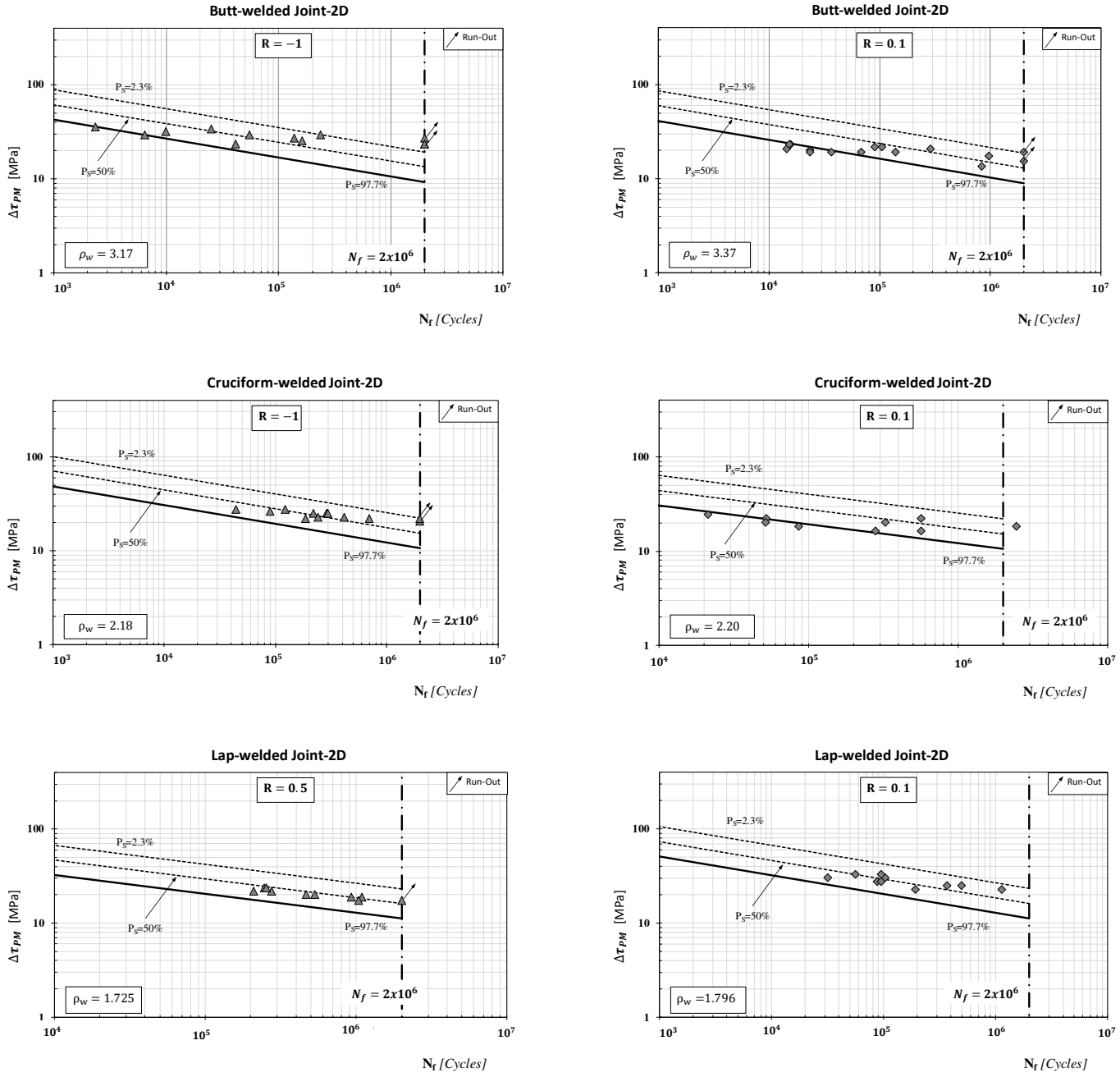

Figure 10. Accuracy of the MWCM applied along with the Point Method in estimating fatigue strength of thin hybrid welded components (2D FE models).

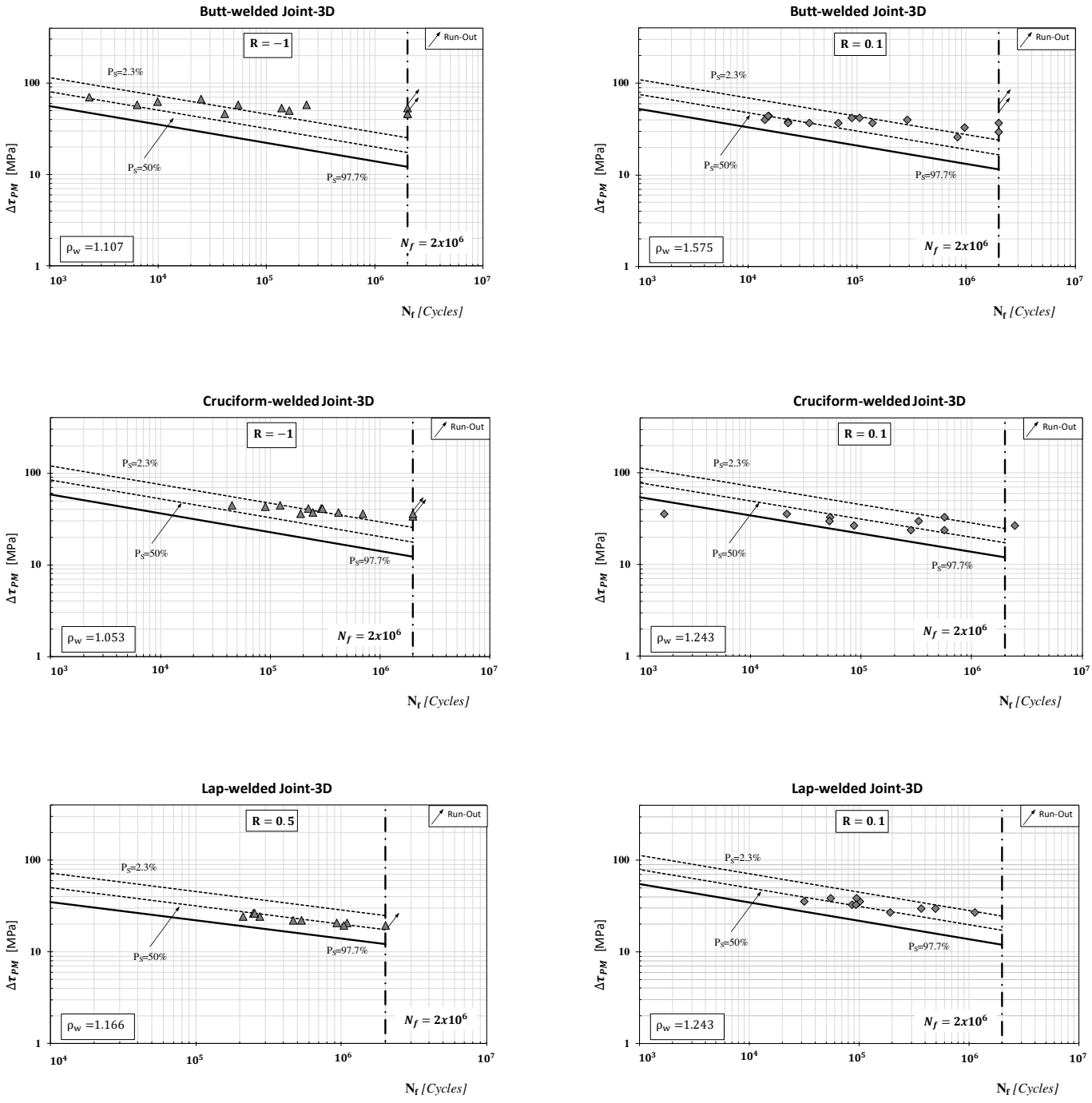

Figure 11. Accuracy of the MWCM applied along with the Point Method in estimating fatigue strength of thin hybrid welded components (3D FE models).